The FEBS Journal

FEBS PRESS science publishing by scientists

EDITOR'S CHOICE

Impaired neural stem cell expansion and hypersensitivity to epileptic seizures in mice lacking the EGFR in the brain

Jonathan P. Robson[1], Bettina Wagner[1], Elisabeth Glitzner[1], Frank L. Heppner[2], Thomas Steinkellner[3], Deeba Khan[4], Claudia Petritsch[5], Daniela D. Pollak[4], Harald H. Sitte[3] and Maria Sibilia[1]

1 Institute of Cancer Research, Department of Medicine I, Comprehensive Cancer Center, Medical University of Vienna, Austria
2 Department of Neuropathology, Cluster of Excellence, NeuroCure, Charité - Universitätsmedizin Berlin, Germany
3 Centre for Physiology and Pharmacology, Institute of Pharmacology, Medical University of Vienna, Austria
4 Centre for Physiology and Pharmacology, Department of Neurophysiology and Neuropharmacology, Medical University of Vienna, Austria
5 Department of Neurological Surgery, UCSF Broad Institute of Regeneration Medicine, University of California San Francisco, CA, USA

Keywords
Epidermal growth factor receptor; epilepsy; glutamate transporter; neural stem cells; neurodegeneration

Correspondence
M. Sibilia, Institute of Cancer Research, Department of Medicine I, Comprehensive Cancer Center, Medical University of Vienna, A-1090 Vienna, Austria
Fax: +43 (0)1 40160 957502
Tel: +43 (0)1 40160 57501
E-mail: maria.sibilia@meduniwien.ac.at

Jonathan P. Robson and Bettina Wagner contributed equally to this work.

(Received 30 April 2018, revised 18 June 2018, accepted 17 July 2018)

doi:10.1111/febs.14603

Mice lacking the epidermal growth factor receptor (EGFR) develop an early postnatal degeneration of the frontal cortex and olfactory bulbs and show increased cortical astrocyte apoptosis. The poor health and early lethality of $EGFR^{-/-}$ mice prevented the analysis of mechanisms responsible for the neurodegeneration and function of the EGFR in the adult brain. Here, we show that postnatal EGFR-deficient neural stem cells are impaired in their self-renewal potential and lack clonal expansion capacity *in vitro*. Mice lacking the EGFR in the brain ($EGFR^{\Delta brain}$) show low penetrance of cortical degeneration compared to $EGFR^{-/-}$ mice despite genetic recombination of the conditional allele. Adult $EGFR^{\Delta}$ mice establish a proper blood–brain barrier and perform reactive astrogliosis in response to mechanical and infectious brain injury, but are more sensitive to Kainic acid-induced epileptic seizures. EGFR-deficient cortical astrocytes, but not midbrain astrocytes, have reduced expression of glutamate transporters *Glt1* and *Glast*, and show reduced glutamate uptake *in vitro*, illustrating an excitotoxic mechanism to explain the hypersensitivity to Kainic acid and region-specific neurodegeneration observed in EGFR-deficient brains.

Abbreviations
Δ, Cre-mediated deletion; AMPAR, α-amino-3-hydroxy-5-methyl-4-isoxazolepropionic acid receptor; BBB, blood–brain barrier; BCA, bicinchoninic acid assay; bFGF, basic fibroblast growth factor; ce, cerebellum; CNS, central nervous system; Co, cortex; EAAT, excitatory amino acid transporters; EGFR, Epidermal Growth Factor Receptor; EPM, elevated plus maze; FACS, fluorescent activated cell sorting; FCS, fetal calf serum; FST, forced swim test; GFAP, glial fibrillary acidic protein; Glast/Eaat1, excitatory amino acid transporter 1; Glt1/Eaat2, excitatory amino acid transporter 2; HB-EGF, heparin-binding EGF-like growth factor; Hi, hindbrain; HRP, horse radish peroxidase; HS, horse serum; KA, kainic acid; LDB, light dark box test; LHRH, luteinizing hormone-releasing hormone; Li, liver; LIF, leukemia inhibitory factor; Mb, midbrain; MK801, dizocilpine; NBQX, 2,3-dihydroxy-6-nitro-7-sulfamoyl-benzo[f]quinoxaline-2,3-dione; Nes, nestin; NMDAR, N-methyl-D-aspartate receptor; Ob, olfactory bulbs; OFT, open field test; PCR, polymerase chain reaction; PDC, L-trans-pyrrolidine-2,4-dicarboxylate; PFA, paraformaldehyde; Prp^{Sc}, infectious prion protein; qPCR, quantitative polymerase chain reaction; RNA, ribonucleic acid; RR, rota rod test; SPT, sucrose preference test; SVZ, subventricular zone; TGF, transforming growth factor; Tl, tail; TST, tail suspension test; VZ, ventricular zone.

Introduction

The epidermal growth factor receptor (EGFR, ErbB1) belongs to a family of receptor tyrosine kinases which are key regulators of embryonic and tumor development [1]. In addition to EGFR, the family includes three additional receptors, ErbB2, ErbB3, and ErbB4. Several ligands have been described for the EGFR, the most prominent being EGF, TGFα, and HB-EGF, while another family of ligands, the neuregulins, are known to bind to ErbB3 and ErbB4. Since there are many different ligands for the ErbB receptors, and the receptors can homo- and heterodimerize, a tremendous diversity of downstream signaling pathways can be initiated in response to different ligand/receptor combinations [2].

In the brain, EGFR expression increases during the late stages of embryonic development and is mainly found in proliferating and migratory regions [3,4]. Increased EGFR expression characterizes a progenitor population in the subventricular zone (SVZ) that is more prone to differentiate into the glial lineage than the neuronal lineage [5]. This bias toward glial differentiation is attributed to synergistic effects of EGF and LIF (leukemia inhibitory factor) [6]. Asymmetric distribution of the EGFR after mitosis of ventricular zone (VZ) and subventricular zone (SVZ) precursors seems to affect cell fate, with a predetermination of the $EGFR^{high}$ population to an astrocytic fate [7]. In the adult brain, EGFR has been shown to play a critical role in the regulation of the neurogenic niches, found in the SVZ of the forebrain and the subgranular zone of the hippocampus [8] [9] [10], where activation of stem cells appears to correlate with the acquisition of EGFR expression [9]. Overexpression of the EGFR in neural precursor cells has been shown to result in reduced neural stem cell proliferation and self-renewal in the SVZ [11], illustrating a critical role of EGFR signaling not only in neural stem cell maintenance but also in astrocyte differentiation.

Complete inactivation of the EGFR gene in mice produces diverse phenotypes depending on the genetic background, ranging from embryonic lethality due to placental defects through to early postnatal mortality from lung immaturity [12–15]. Mice surviving the first postnatal week are growth retarded and show abnormalities in skin [12,14,15], bone [16,17], intestine [12] and brain [13,15,18] development, proving an essential role for EGFR signaling in multiple organs. Most EGFR knock-out mice die before weaning age, although in very rare cases the mice can survive up to 1 month [12,14]. Embryonic brain development proceeds inconspicuously in EGFR knock-out mice, but postnatally a massive degeneration of the cerebral cortex and the olfactory bulbs can be observed, which is characterized by apoptotic death of neurons as well as astrocytes [13,18]. Degenerative processes can also be detected in the thalamus but thalamic astrocytes do not seem to be affected by apoptosis and can actively respond to the neuronal degeneration by inducing reactive gliosis. Interestingly, cultured cortical astrocytes, but not midbrain astrocytes from EGFR knock-out mice, are more susceptible to apoptosis than astrocytes from other brain regions, a phenomenon paralleled by decreased activation of Akt in cortical knock-out astrocytes [19]. Moreover, EGFR-deficient cortical astrocytes cannot support neuronal survival in an *in vitro* coculture system between astrocytes and neurons suggesting that defects in cortical astrocytes might be responsible for the cortical neurodegeneration observed *in vivo* [19].

Astrocytes are one of the critical differentiated cell types of the brain that primarily have a protective function, forming the tripartite synapse along with the pre- and postsynaptic neurons. Astrocytes ensure correct homeostasis of excitatory neurotransmitters and dysregulation of astrocyte function has been associated with seizures and epileptogenesis [20]. This homeostasis is largely controlled via neurotransporters, which take up excess neurotransmitters within the synaptic cleft. The primary excitatory neurotransmitter in the mammalian brain is glutamate, which is regulated by glutamate transporters (excitatory amino acid transporters; EAAT1-5), of which Eaat2 (Glt1) and Eaat1 (Glast) are the two most prominent and expressed on astrocytes [21,22]. Glutamate transporters on glial cells have been shown to account for the majority of glutamate uptake in the brain, and impaired glutamate uptake by these transporters has been shown to contribute to the development of epilepsy [23,24].

To investigate the role of EGFR in the adult brain, we generated two conditional EGFR-deficient mouse models where Cre recombinase is driven by the Nestin [25] or GFAP [26] promoter. Here, we report that mice with brain-specific ablation of EGFR do not display significant brain phenotypes but are severely susceptible to Kainic acid-induced epilepsy. Furthermore, in the absence of EGFR we identified a defective glutamate transport activity in cortical EGFR-deficient astrocytes proposing a neurotoxicity basis for the neurodegeneration observed in EGFR-deleted brains. We therefore identified a critical role of EGFR signaling for the survival and functionality of cortical astrocytes and neurons through glutamate transport regulation.

Results

EGFR-deficient neural stem cells show a lack of symmetric stem cell division *in vitro*

The EGFR$^{-/-}$ mice have previously been reported to have severe developmental defects. Our EGFR$^{-/-}$ model supports these previous data and show defects including a bulging eye phenotype (Fig. 1A) and neocortex neurodegeneration (Fig. 1B). In EGFR$^{-/-}$ mice, neurodegeneration was frequently presented as a profound loss of NeuN+ neurons in the dorsal cortex associated with GFAP+ astrogliosis (Fig. 1C,D). EGFR signaling has been well reported to be important in the maintenance of neural stem cells [11,27–30]. We wanted to investigate whether postnatal EGFR-deficient neural stem cells were impaired, which could account for any extensive developmental defects observed throughout development. To this end we isolated cells from the cortical neurogenic niche, the subventricular zone (SVZ), from P2 EGFR$^{+/+}$ and EGFR$^{-/-}$ brains ($n = 4$). Initial plating of neurogenic cells under neurosphere growing conditions (termed the sphere forming unit assay, SFUA) identified a reduced neurosphere forming potential in EGFR$^{-/-}$ mice compared with controls (Fig. 2A). Specifically, EGFR$^{-/-}$-derived primary cells were critically dependent on bFGF for survival and/or expansion ($P < 0.0001$), corroborating a previous study where we have shown that embryonic SVZ cells can expand in the presence of bFGF [30].

Clonal expansion of the plated cells as free-floating neurospheres allows for the analysis of stem cell division, shown as an expanding population following sequential passaging, indicating that the primary neurogenic cells are capable of self-renewal and proliferation. EGFR$^{+/+}$-derived neurospheres were able to clonally expand in the presence of EGF ($n = 6$) or EGF+bFGF ($n = 6$) while bFGF alone ($n = 5$) allowed only for the survival of progenitor cells (Fig. 2B,C). Interestingly, EGFR$^{-/-}$-derived neurospheres showed a complete inability of clonal expansion when cultured with EGF ($n = 5$) or bFGF ($n = 5$) (Fig. 2B,D). Differentiation of EGFR$^{+/+}$ or EGFR$^{-/-}$ neurospheres

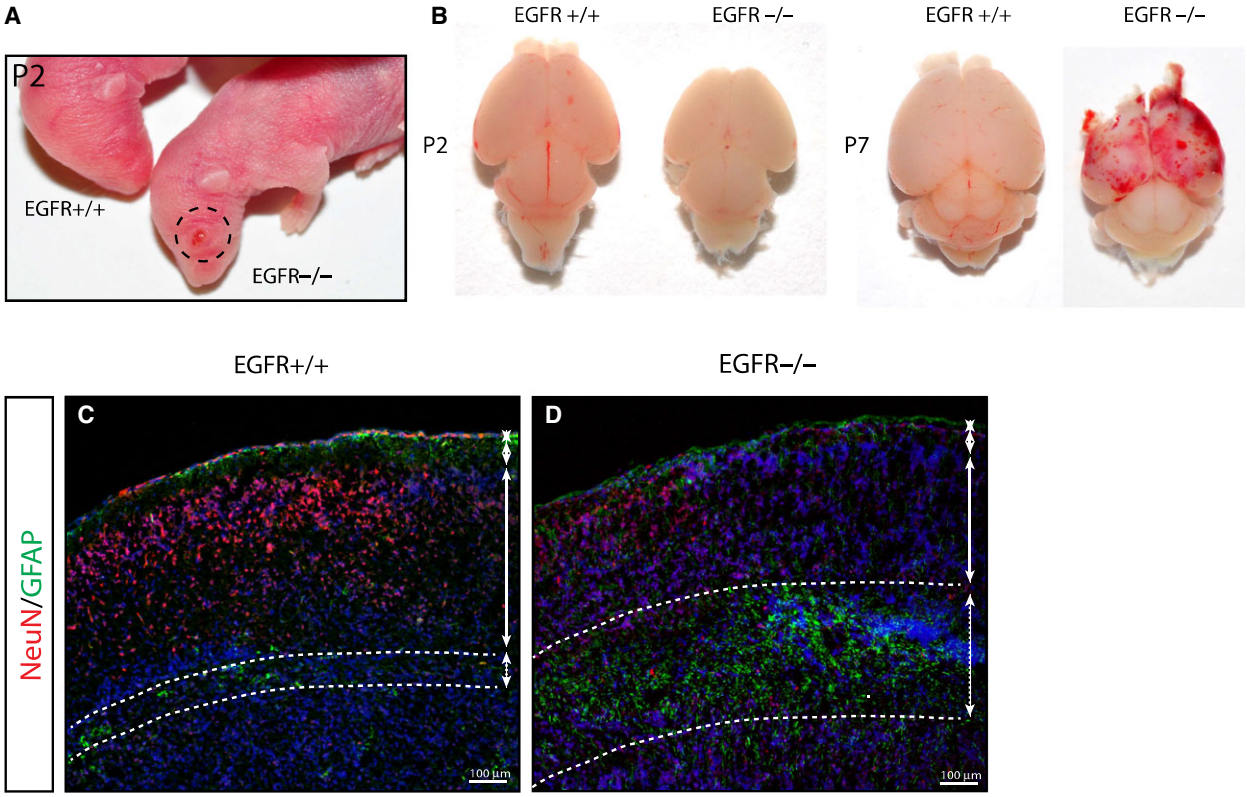

Fig. 1. EGFR knock-out mice display neurodegeneration (A) EGFR$^{-/-}$ newborn mice display an open-eye phenotype (dotted circle). (B) Whole images of brains isolated from P2 and P7 EGFR knock-out mice (EGFR$^{-/-}$) and littermate controls illustrate reduced brain size in EGFR$^{-/-}$ mice. By P7 the majority (but not all) EGFR$^{-/-}$ brains show a bloody frontal cortex. (C, D) Concomitant with a loss of NeuN+ neurons is an increase in GFAP+ cells in P6 EGFR$^{-/-}$ mice compared with littermate controls.

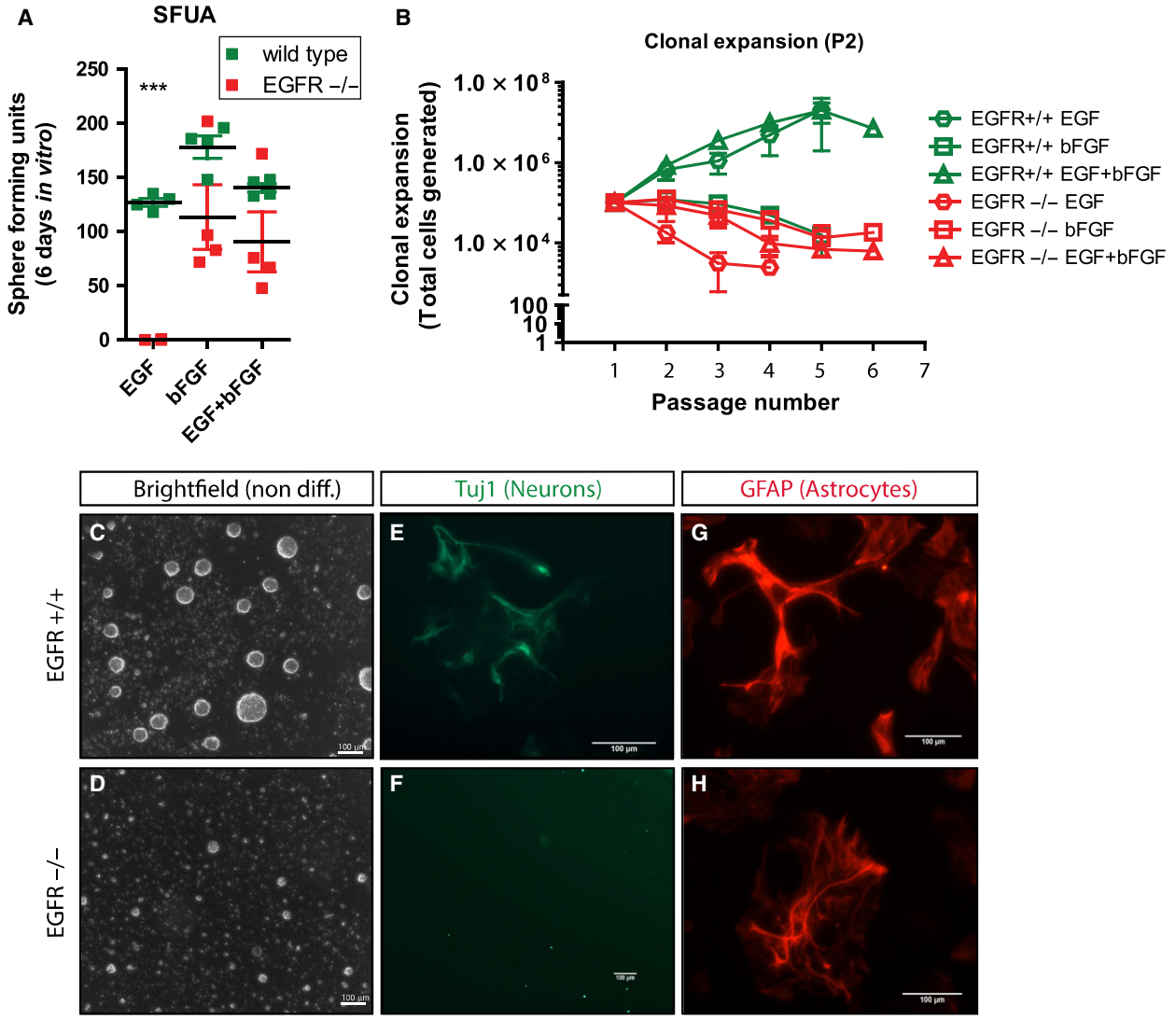

Fig. 2. EGFR ablated neural stem cells show a lack of clonal expansion *in vitro*. (A) Primary sphere forming unit assay (SFUA). Primary EGFR-deficient cells isolated from the cortex neurogenic niche, the subventricular zone, show reduced sphere forming potential compared to wild-type cells when cultured with bFGF or bFGF+EGF and show complete inability to form spheres when cultured with EGF alone ($n = 4$). (B) Neurosphere clonal expansion assay. A continuation from the SFUA, prolonged cultivation of WT or EGFR$^{-/-}$ stem-like cells as neurospheres shows clonal expansion, and thus confirmation of symmetric stem cell division, in WT spheres (C) cultured with EGF alone ($n = 6$) or EGF+bFGF ($n = 6$) but not with bFGF alone ($n = 5$). In contrast, EGFR$^{-/-}$ spheres (D) are unable to clonally expand in the presence of EGF ($n = 5$) or bFGF ($n = 5$). (E–H) Differentiation assay of WT and EGFR$^{-/-}$ neurospheres. Under serum addition and growth factor removal conditions WT spheres could differentiate into neurons and astrocytes while EGFR$^{-/-}$ spheres would only differentiate into astrocytes and not neurons. Error bars indicate SEM; *** indicates $P < 0.0005$ (*t*-test with welches correction).

identified a normal capacity of WT neurospheres to differentiate into neurons and astrocytes (Fig. 2E,G) while EGFR$^{-/-}$ neurospheres would only differentiate into GFAP+ astrocytes (Fig. 2F,H). Collectively, this data illustrate that EGFR$^{-/-}$ SVZ-derived cells lack the ability to undergo clonal expansion and preferentially differentiate into astrocytes *in vitro*. These results suggest that complete loss of EGFR in the SVZ neurogenic niche results in a reduced clonal expansion capacity of neural stem cells and promotes specification to a glial lineage progenitor cell.

EGFR$^{\Delta Nes}$ and EGFR$^{\Delta Gfap}$ mice show growth retardation and low penetrance of cortical degeneration during early postnatal development

To better investigate the role of EGFR in adult brain development we bred mice with a conditional EGFR

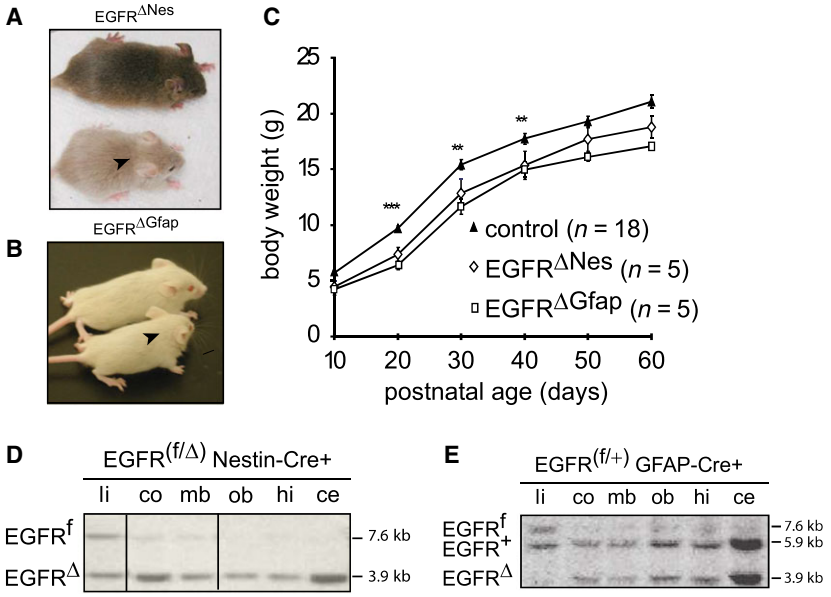

Fig. 3. EGFR$^{\Delta}$ mice are smaller than littermate controls. Gross size differences were visible between EGFR$^{\Delta Nes}$ (A) and EGFR$^{\Delta Gfap}$ (B) mice (arrow heads) and their respective control littermates. (C) Postnatal weight gain of wild-type (n = 18) and EGFR$^{\Delta Nes}$ (n = 5) and EGFR$^{\Delta Gfap}$ (n = 5) mice. Results represent the mean weight ± SEM of females from at least 3 litters. Error bars indicate SEM; ***P <0.005, **P <0.05. (D, E) Southern blot analysis of genomic DNA isolated from different brain regions of an EGFR$^{f/\Delta}$ Nestin-Cre^{+} (D) and EGFR$^{f/+}$ GFAP-Cre^{+} (E) mouse. Because in EGFR$^{f/\Delta}$ mice the Δ allele (resulting from germline Cre deletion) was inherited from the parents, it is present in all tissues including the liver that is used as control tissue. Nes-Cre and GFAP-cre are not expressed in the liver and thus the floxed allele is also visible, while in the brain the floxed allele is recombined giving rise to the Δ allele. EGFR$^{f/+}$ mice, which have no germline deletion of EGFR, show only the floxed alleles where cre-mediated deletion can occur.

allele (floxed EGFR allele; EGFR^{f}) [31] with two brain-specific Cre lines with slightly different temporal and spatial expression profiles. Cre recombinase expression from the rat nestin promoter [25] was used to induce recombination of the EGFR^{f} allele in all cells of the central nervous system (EGFR$^{\Delta Nes}$), beginning from approximately E14.5. Additionally, we used mice expressing the Cre recombinase under the mouse GFAP promoter [26] to trigger recombination of the EGFR^{f} allele, mainly in astrocytes (EGFR$^{\Delta Gfap}$), from approximately E16.5. Cre recombinase is also active in ependymal cells and some neurons in this Cre line [26]. Although the spectrum of EGFR deletion was similar with both Cre lines, the analyses that follow were performed with both lines to corroborate the findings in two different models.

EGFR$^{\Delta Nes}$ and EGFR$^{\Delta Gfap}$ mice (collectively called EGFR$^{\Delta}$) were born at the expected Mendelian frequencies and were indistinguishable from their respective control littermates at birth. However, after the first postnatal week size differences between EGFR$^{\Delta Nes}$ and control mice became apparent, with EGFR$^{\Delta Nes}$ mice being explicitly smaller than their littermates (Fig. 3A). Similar size differences were also observed for EGFR$^{\Delta Gfap}$ mice (Fig. 3B). At weaning EGFR$^{\Delta Nes}$ (n = 5) and EGFR$^{\Delta Gfap}$ (n = 5) mice weighed ~ 20% less than control mice (n = 18) and remained significantly smaller (at 4–6 months of age Nes controls 33.43 g ± 1.97, EGFR$^{\Delta Nes}$ 24.70 g ± 0.32, P = 0.012; Gfap Controls 32.53 g ± 1.23, EGFR$^{\Delta Gfap}$ 24.94 g ± 0.85, P < 0.0001) (Fig. 3C). No gross neurological differences were observed between models and both strains of mice were fertile and lived a normal lifespan.

The midbrain, olfactory bulbs, hindbrain and cerebellum all showed recombination of the EGFR allele in both EGFR$^{\Delta Nes}$ and EGFR$^{\Delta Gfap}$ mice at birth (Fig. 3D,E). In addition, Southern blot analysis revealed that most of the EGFR^{f} allele is recombined in both EGFR$^{\Delta Nes}$ and EGFR$^{\Delta Gfap}$ cortices at birth (postnatal day 0; P0) (Fig. 4A). At P9 EGFR protein could still be detected in the cortex of EGFR$^{\Delta Nes}$ mice by western blot (Fig. 4B). The EGFR$^{\Delta Nes}$ model was chosen because of the more complete recombination of the conditional EGFR allele. Although the amount was clearly diminished compared to a control cortex, it was probably sufficient to guarantee basic EGFR functions. Even at weaning age (P24) residual EGFR protein was detectable in EGFR$^{\Delta Nes}$ cortices (Fig. 4B). These results indicate that in the early postnatal period some EGFR protein is still present in the brain of EGFR$^{\Delta Nes}$ mice, which may account for the absence of neurodegeneration.

External analysis of the eyes of $EGFR^{\Delta Nes}$ and $EGFR^{\Delta Gfap}$ mice identified no obvious abnormalities (Fig. 4C), which, in contrast, were always observed in $EGFR^{-/-}$ mice (Fig. 1A). Gross analysis of brains from $EGFR^{\Delta Gfap}$ (Fig. 4D) and $EGFR^{\Delta Nes}$ (Fig. 4E) mice showed that these brains were smaller than those from control mice. The differences in brain size were comparable to the size differences observed in $EGFR^{\Delta Nes}$ and $EGFR^{\Delta Gfap}$ versus control mice but did not display any external signs of degeneration. In $EGFR^{-/-}$ mice degeneration of the frontal cortex is macroscopically detectable in the second postnatal week, when large parts of the upper cortical layers have degenerated, usually concomitant with a bloody frontal cortex by ~ P7 (Fig. 1B) [19]. To further analyze whether brain development was defective in $EGFR^{\Delta}$ mice, brains were sectioned and analyzed by immunohistochemistry. Hematoxylin and Eosin staining of sagittal sections showed that the structure of the main brain regions was comparable between $EGFR^{\Delta Nes}$, $EGFR^{\Delta Gfap}$ and control mice (Fig. 4F–K). In $EGFR^{-/-}$ mice, neurodegeneration is frequently presented as a profound loss of NeuN+ neurons in the dorsal cortex associated with GFAP+ astrogliosis (Fig. 1C,D). Staining with neuronal markers did not reveal any significant differences in cortical organization and cortical lamination between $EGFR^{\Delta Gfap}$ and control mice (Fig. 4L, M) indicating that no degenerative processes were occurring in the majority of these mice. Therefore, it seems that cortical development is not compromised in $EGFR^{\Delta}$ mice. However, upon analysis of more $EGFR^{\Delta Nes}$ mice it became apparent that a small number of these mice (less than 5%) exhibited partial cortical degeneration with destruction of laminar patterns (Fig. 4N), similar to the degeneration observed in $EGFR^{-/-}$ mice.

To investigate whether $EGFR^{\Delta}$ mice had any behavioral abnormalities they were subjected to an array of behavioral analyses. All tests were carried out on male adult mice (4–6 months of age). While some differences were observed between $EGFR^{\Delta Gfap}$ ($n = 13$) and controls ($n = 11$) in the Elevated Plus Maze (Fig. 5A, B,C: 5.0-fold increased percent entries in open arms, $P = 0.004$; 2.94-fold increased percent time in open arms, $P = 0.050$; 3.28-fold increased percent distance, $P = 0.046$), Rota Rod test (Fig. 5D: 1.8-fold increased latency, $P = 0.047$), and Tail Suspension Test (Fig. 5M: 1.56-fold increased percent time spent immobile, $P = 0.014$) the remaining studies showed no significant differences between groups (Fig. 5). $EGFR^{\Delta Nes}$ mice ($n = 3$) showed no statistical differences to controls ($n = 3$) in all tests save the Elevated plus maze test (Fig. 5A: 2.23-fold increased percent entries in open arms, $P = 0.037$). While single results of the behavioral analysis suggest some alterations in emotional behavior and motor coordination, these observations were not confirmed in other tests suggesting that conditional EGFR deletion in the mammalian brain does not affect behavior.

Aside from the cortex we also analyzed other brain regions affected in the $EGFR^{-/-}$ mice. We have previously reported that the thalamus of $EGFR^{-/-}$ mice was also affected by degenerative processes, which are accompanied by massive astrogliosis [13]. Neither neuronal loss nor increased astrogliosis could be observed in the thalami of $EGFR^{\Delta Nes}$ and $EGFR^{\Delta Gfap}$ mice, however, closer inspection of the hippocampi revealed the presence of nests of ectopic neurons in the white matter both in $EGFR^{\Delta}$ mice (Fig. 6A–C), a phenotype previously observed also in $EGFR^{-/-}$ mice [13]. These findings were further confirmed via Bielschowsky staining which showed the presence of unmyelinated axons and neuronal plaques in the regions above the ectopic neurons (Fig. 6D-F). Collectively these results show that $EGFR^{\Delta Nes}$ and $EGFR^{\Delta Gfap}$ mice have smaller brains that are generally normal on a histological scale, albeit with rare neurodegeneration.

Absence of the EGFR in brain cells does not affect blood–brain barrier function, astrogliosis, or response to pathogenic insult

An intact blood–brain barrier (BBB) ensures brain homeostasis by efficiently preventing molecules from

Fig. 4. Nestin-Cre and GFAP-Cre-mediated deletion of EGFR results in a grossly normal neocortex with rare neurodegeneration. (A) Southern blot analysis of EGFR recombination in cortices of $EGFR^{\Delta Gfap}$ and $EGFR^{\Delta Nes}$ mice at birth (P0). An EGFR- knock-out allele and an EGFR flox allele can be observed as the $EGFR^{\Delta Gfap}$ and $EGFR^{\Delta Nes}$ mice were breed with conventional EGFR knock-out mice to ensure Cre-mediated deletion of the floxed allele. Tail-DNA from the respective mice (tl) were used as controls. (B) Western blot analysis showing expression of EGFR protein in the cortices of $EGFR^{\Delta Nes}$ mice at postnatal day 9 and 24. (C) No occular phenotypes were observed in adult $EGFR^{\Delta Nes}$ or $EGFR^{\Delta Gfap}$ mice compared to control mice. (D, E) Brains from $EGFR^{\Delta Nes}$ or $EGFR^{\Delta Gfap}$ are smaller than those from control littermates but show no obvious cortical degeneration. (F–K) Histological sections show normal cortical organization in $EGFR^{\Delta Gfap}$ (G) and $EGFR^{\Delta Nes}$ (H) cortices compared to control cortices (F); to allow a better representation of cortical lamination a higher magnification of the cortices shown in (F), (G), (H) are shown in (I), (J), (K), respectively; cortical degeneration is visible in some $EGFR^{\Delta Nes}$ mice (N). (L, M) Immunofluorescent staining for NeuN in $EGFR^{\Delta Gfap}$ and control cortices. Neurons (NeuN+) appear unaffected in $EGFR^{\Delta Gfap}$ cortices compared with controls. NC, neocortex; CA1, hippocampal cornu ammonis area 1; I–VI, cortical layers I–VI. Abbreviations in (A) co, cortex; ce, cerebellum; hi, hindbrain; li, liver; mb, midbrain; ob, olfactory bulbs.

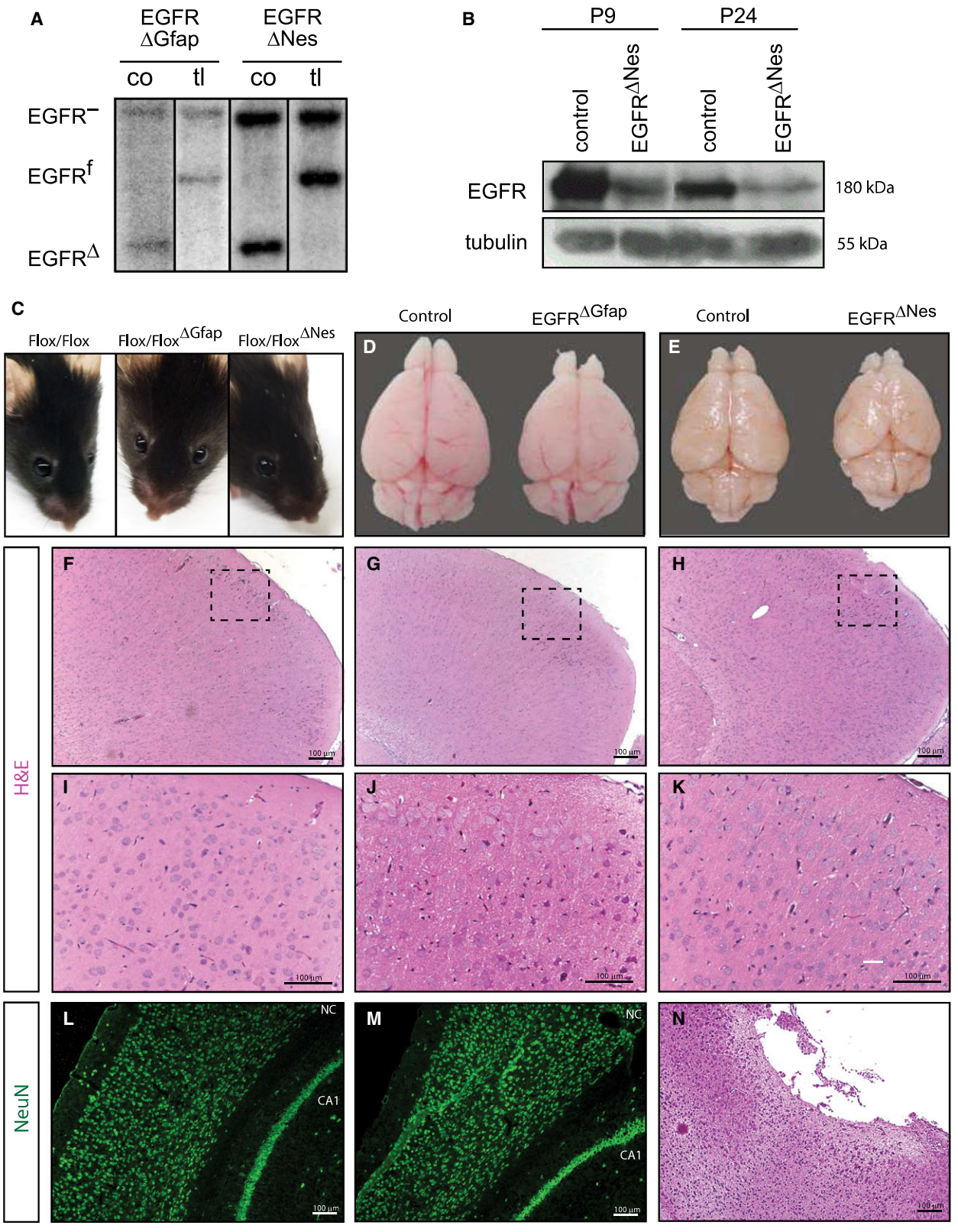
A
EGFR ΔGfap
EGFR ΔNes
co
tl
co
tl
EGFR⁻
EGFR^f
EGFR^Δ
B
P9
P24
control
EGFR^ΔNes
control
EGFR^ΔNes
EGFR
180 kDa
tubulin
55 kDa
C
Flox/Flox
Flox/Flox^ΔGfap
Flox/Flox^ΔNes
Control
EGFR^ΔGfap
Control
EGFR^ΔNes
D
E
H&E
F
G
H
I
J
K
100 µm
NeuN
L
M
N
NC
CA1

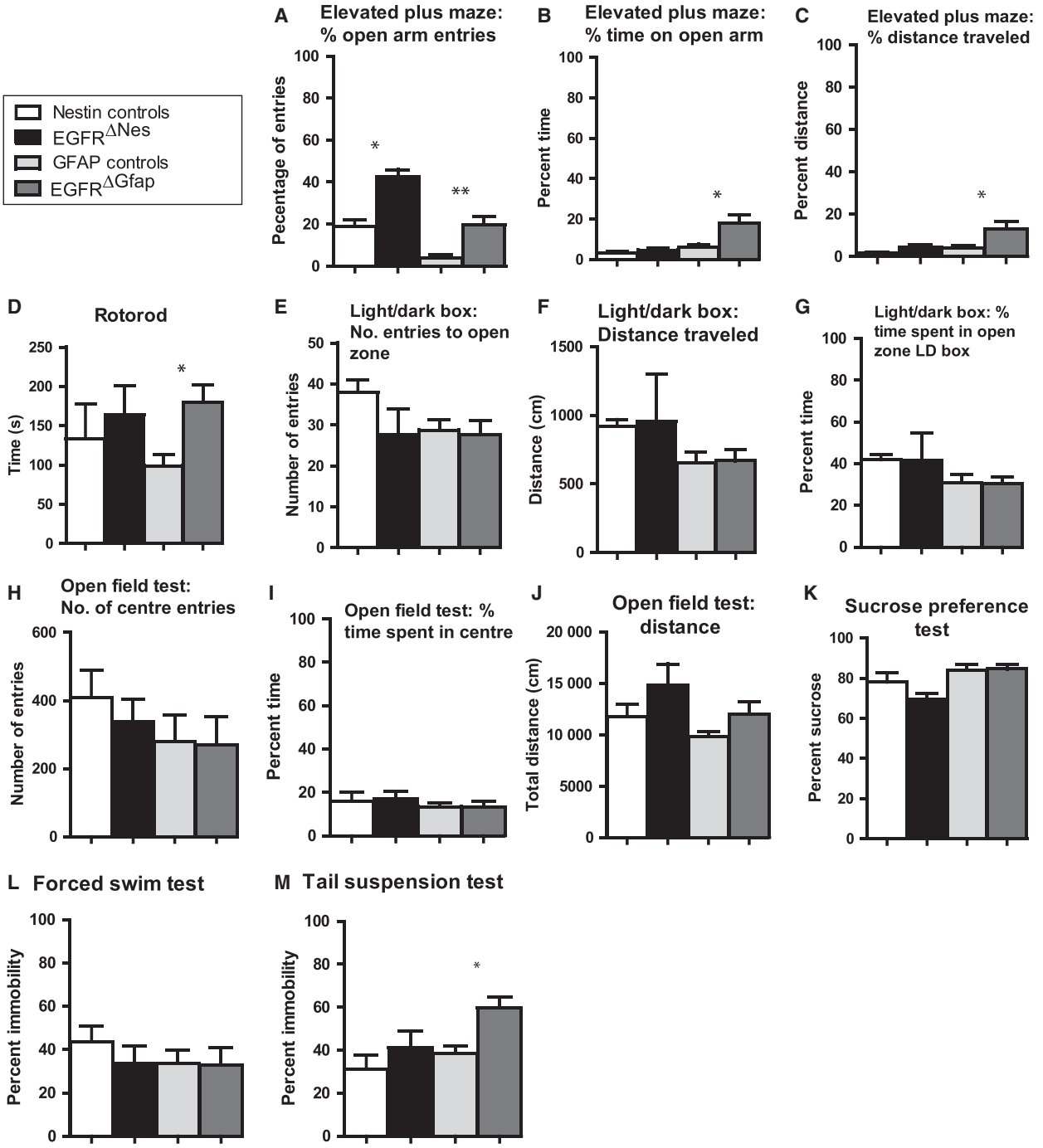

Fig. 5. EGFR$^{\Delta}$ mice display no gross behavioral differences. (A–M) Behavioral studies on EGFR$^{\Delta Nes}$, EGFR$^{\Delta Gfap}$ and littermate control mice. While some differences were observed between EGFR$^{\Delta Gfap}$ (n = 13) and controls (n = 11) in the Elevated plus maze test (A–C), Rotarod test (D) and tail suspension test (M) the remaining studies showed no significant differences between genotypes. EGFR$^{\Delta Nes}$ mice (n = 3) showed no statistical differences to controls (n = 3) in all tests save the Elevated plus maze test (A). All data are displayed as mean ± SEM; *= $P < 0.05$, **= $P < 0.005$; statistical significance calculated using one-way ANOVA with *post hoc* analysis.

entering the brain [13]. Astrocytes are known to be important in BBB formation by inducing endothelial cells to form the tight junctions characteristic of the BBB [32]. Given EGFR plays an important role in regulating astrocyte proliferation/differentiation, we wanted to determine whether the absence of EGFR

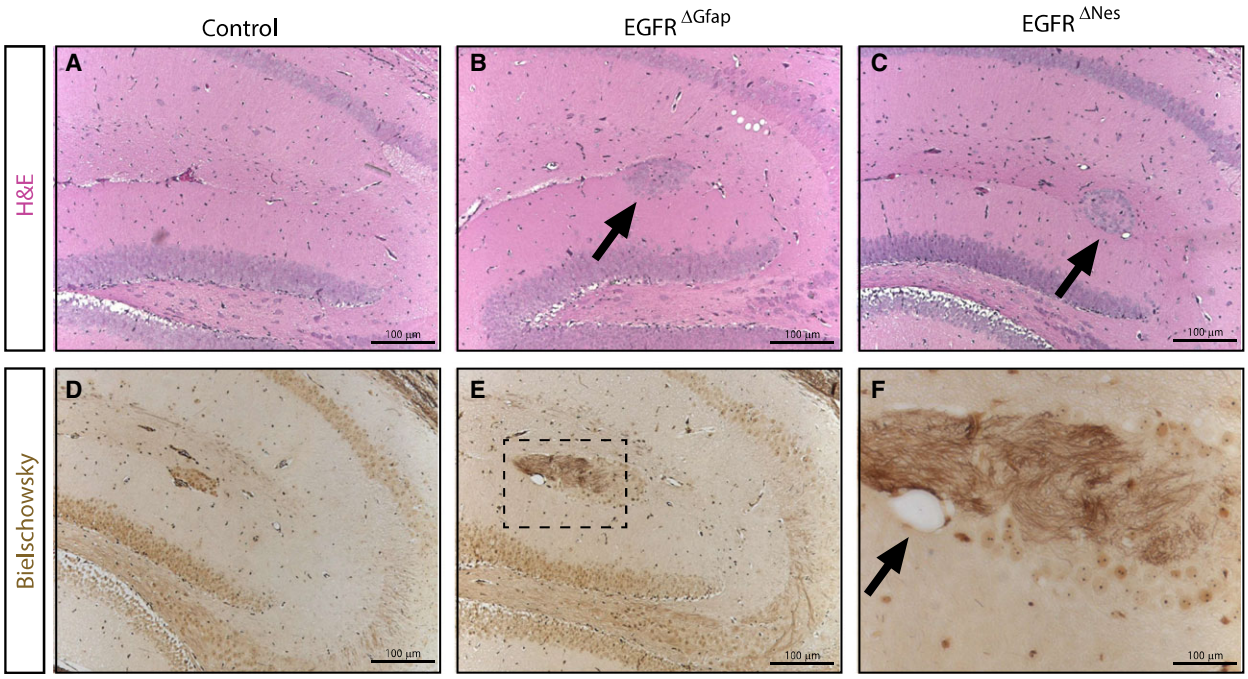

Fig. 6. EGFR$^{\Delta}$ brains show ectopic neuron formation in the hippocampus. Nests of ectopic neurons are present in the white matter of the hippocampi in EGFR$^{\Delta Gfap}$ and EGFR$^{\Delta Nes}$ mice. Histological sections of the hippocampi of either control (A), EGFR$^{\Delta Gfap}$ (B) or EGFR$^{\Delta Nes}$ mice (C). (D–F) Bielschowsky stainings of the hippocampus from an EGFR$^{\Delta Nes}$ mouse. (D) and (E) represent images from different lateral positions of the same hippocampus. (F) shows a magnification of the boxed region in (E). Arrows in (B, C) indicate nests of ectopic neurons; (F) indicate neuronal plaques.

in brain cells affects BBB function. To evaluate the integrity of the BBB, EGFR$^{\Delta Nes}$ mice were injected intravenously with HRP. In the case of BBB malfunction the HRP would leak into the brain and HRP substrate-specific staining would be detectable. Mice whose BBB was opened in response to a stab-wound injury, which were used as positive controls, showed extensive HRP substrate-specific staining around the wound (Fig. 7B). No HRP signal was observed in the brains of EGFR$^{\Delta Nes}$ (Fig. 7C), EGFR$^{\Delta Gfap}$ (Fig. 7D) or control (Fig. 7A) mice, indicating that in adult mice BBB function is not affected by the absence of EGFR.

A prominent function of astrocytes is their role in response to brain injuries, a process termed reactive astrogliosis. During astrogliosis astrocytes become hypertrophic, upregulate GFAP expression and secrete different sets of molecules [33]. In severe cases of trauma astrocytes proliferate and migrate to the injured region, where they initiate the formation of scar tissue. The EGFR ligands TGFα and EGF are implicated in the induction and proliferation of reactive astrocytes [34,35]. To determine whether the absence of the EGFR in the brain of adult mice results in functional impairment of astrogliosis, either by inhibiting astrocyte migration or by altering the composition of secreted factors, we analyzed the cellular response to traumatic brain injury. Adult mice older than 3 months were used to ensure the complete absence of the EGFR in the brain. Forebrain stab injuries were performed as previously described [36] and mice were sacrificed 1 and 5 weeks after injury to analyze wound healing. One week after the insult wounds were not completely closed irrespective of the genotype, and comparable numbers of infiltrating astrocytes were detected in EGFR$^{\Delta Gfap}$, EGFR$^{\Delta Nes}$, and control mice (Fig. 7E,I,M). Thirty-five days after injury the wounds were closed in all genotypes and a glial scar had developed (Fig. 7G, K,O). GFAP-positive reactive astrocytes were observable at 7 days (Fig. 7F,J,N) and still detectable around the scar at 35 days postwounding, indicating ongoing regeneration (Fig. 7H,L,P). We were not able to detect differences concerning the quality of the glial scar or the time required for healing between the genotypes. These results indicate that EGFR signaling is dispensable for astrogliosis and brain injury repair.

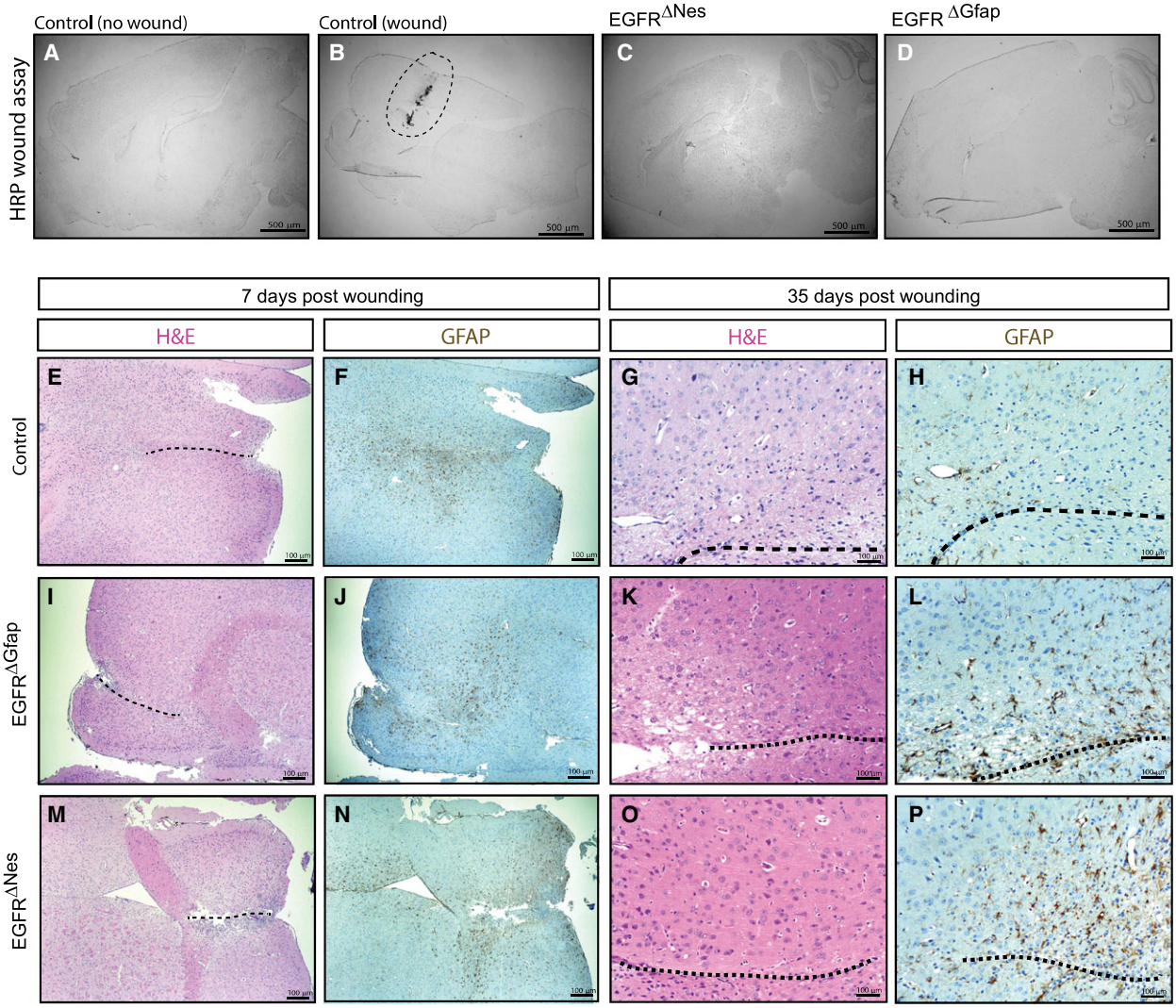

Fig. 7. Absence of EGFR in brain cells does not impair astrogliosis or affect the response to pathogenic insults (A–D). HRP stab wound assay of EGFR$^{\Delta}$ mice. No HRP-specific substrate staining was observed in (A) control brains, (C) EGFR$^{\Delta Gfap}$ brains or (D) EGFR$^{\Delta Nes}$ brains but HRP-specific substrate staining is clearly visible in (B) stab wound control brains (dotted circle). (E–P) Wound healing and astrogliosis are not impaired in EGFR$^{\Delta Gfap}$ and EGFR$^{\Delta Nes}$ brains; Histological sections of adult brains 7 days and 35 days postwounding (dotted lines) stained for Hematoxylin & Eosin or GFAP. Images (E–H) show a control brain, while (I–L) and (M–P) show sections from an EGFR$^{\Delta Gfap}$ and an EGFR$^{\Delta Nes}$ brain, respectively.

Since EGFR expression in astrocytes does not seem to be essential for acute injury responses, we next evaluated whether absence of the EGFR affects the response to a chronic pathogenic challenge in the brain. A well-characterized model for such a challenge is prion disease, where brains of mice infected with prion protein develop pathological changes within 150–200 days after infection which, at the histological level, are manifested by accumulation of infectious prion protein (Prp^{Sc}), development of astrogliosis and neuronal loss [37]. EGFR$^{\Delta Gfap}$, EGFR$^{\Delta Nes}$, and control mice were intracerebrally infected with two different doses of the RML5 strain of murine adapted scrapie prions. Regardless of their genotype all animals showed comparable symptoms of prion disease and succumbed to the disease after the same incubation period (low dose: EGFR$^{\Delta Gfap}$ 193 ± 16 days (n = 7), EGFR$^{\Delta Nes}$ 207 ± 9 days (n = 7), control 202 ± 13 days (n = 6); high dose: EGFR$^{\Delta Gfap}$ 170 ± 11 days (n = 6), EGFR$^{\Delta Nes}$ 170 ± 13 days (n = 4), control 176 ± 7 days (n = 4)) (Fig. 8A,B). Histological analysis revealed the hallmarks of prion disease such as extensive neuronal loss (Fig. 8C,F,I), and accumulation of prion protein (Fig. 8E,H,K). Astrogliosis characterized by increased

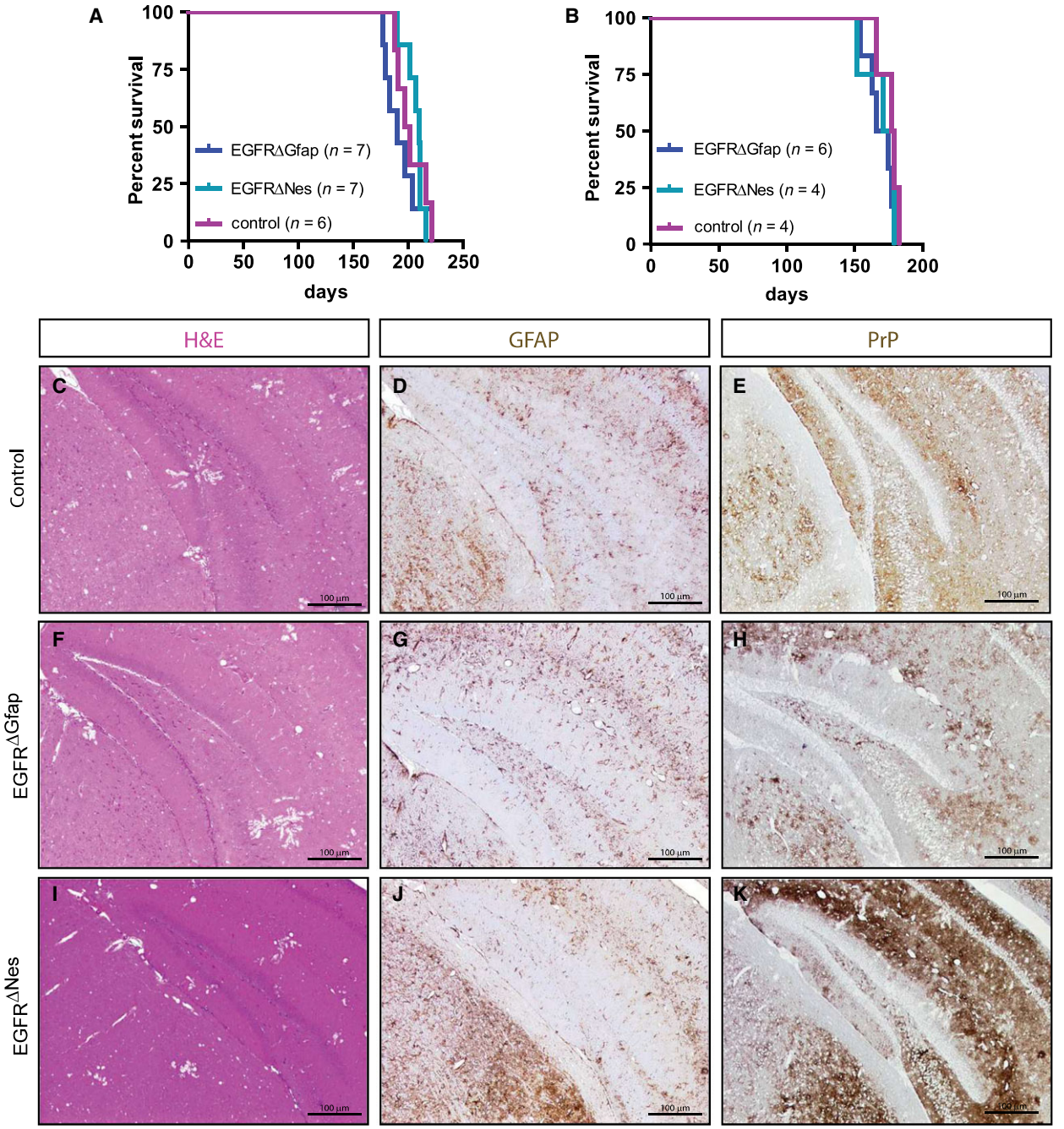

Fig. 8. Prion infection assay. (A, B) The response to Prion-induced insults is not impaired in EGFR$^{\Delta Nes}$ and EGFR$^{\Delta Gfap}$ mice. Kaplan–Meier plots showing the survival of EGFR$^{\Delta Nes}$ and EGFR$^{\Delta Gfap}$ mice compared to controls after intracerebral prion inoculation using either a low dose (A; n = 6–7) or a high dose (B; n = 4–6) of RML5. (C–K) Comparable neuropathological changes in the hippocampi of control (C–E), EGFR$^{\Delta Gfap}$ (F–H) and EGFR$^{\Delta Nes}$ (I–K) mice following pathogenic insult from prion infection. Spongiform changes were visualized with Hematoxylin and Eosin staining (C, F, I) and astrocyte responses were analyzed with GFAP staining (D, G, J). Immunohistochemistry against PrP showed equivalent staining in all genotypes (E, H, K). Scale 100 µm.

amounts of highly GFAP-positive cells were also observed irrespective of the genotype (Fig. 8D,G,J). Together with the traumatic brain injury results these experiments indicate that EGFR function may contribute to, but is not strictly required for initiating a response to brain injuries.

Absence of EGFR in brain cells increases susceptibility to Kainic acid-induced epilepsy

We have previously reported that cortical neuron survival is impaired in EGFR ablated mice [19]. In addition to investigating the role that loss of EGFR has with traumatic brain injury we wanted to determine if EGFR ablated brains are susceptible to neurotoxicity-induced neuronal death. One model routinely used to investigate such phenomenon is the triggering of seizures with Kainic acid (KA), a marine-derived amino acid that has a very high activating potential of glutamate transporters [38–41]. Several molecules acting downstream of the EGFR have been implicated in mediating KA-induced neurotoxicity [42,43]. KA elicits seizures by direct stimulation of glutamate receptors, and indirectly by increasing the release of excitatory amino acids from nerve terminals [40]. We wanted to determine whether the absence of EGFR signaling affects the responses to glutamatergic stimulation in the brain. Mice were injected intraperitoneally with KA at a dose of 25 mg·kg^{-1} body weight. The KA-elicited seizures were measured over a period of 120 min and were classified according to their intensity within the first 25 min ranging from stage 1–6 as previously described [44]. Stage 1 is rated as arrest of motion and the seizure level gradually increases to level 6, which is characterized by generalized tonic–clonic activity with loss of postural tone or death. KA treatment resulted in seizures in both EGFR$^{\Delta Nes}$ and mice EGFR$^{\Delta gfap}$, as well as their control littermates (WT). Severe seizures were observed in EGFR$^{\Delta Nes}$ mice ($P = 0.0001$; Fig. 9A), and to a lesser degree in EGFR$^{\Delta Gfap}$ mice ($P = 0.07$; Fig. 10A). EGFR$^{\Delta Nes}$ mice seizures exhibited a progressive severity resulting in generalized tonic–clonic activity with loss of postural tone and death within 25 min after KA treatment ($n = 9$; Fig. 9A). Nine of the 12 Nestin littermate control mice survived the KA-induced epilepsy, while 9/9 EGFR$^{\Delta Nes}$ mice died within 30 min ($P =< 0.0001$; Fig. 9B). Gfap littermate control mice displayed more varied results with three of five mice surviving while five of five EGFR$^{\Delta Gfap}$ mice died within 80 min ($P = 0.035$; Fig. 10B).

To determine if the seizures generated in EGFR-ablated mice could be ameliorated by glutamate receptor antagonists we pretreated mice with either the NMDAR antagonist MK801 or the AMPAR antagonist NBQX prior to KA injection. Pretreatment with MK801 significantly ameliorated epileptic seizures in Nestin littermate control mice (median seizure score 1.5, $P = 0.013$; $n = 3$; Fig. 9A) while no significant effects were observed in EGFR$^{\Delta Nes}$ mice (median

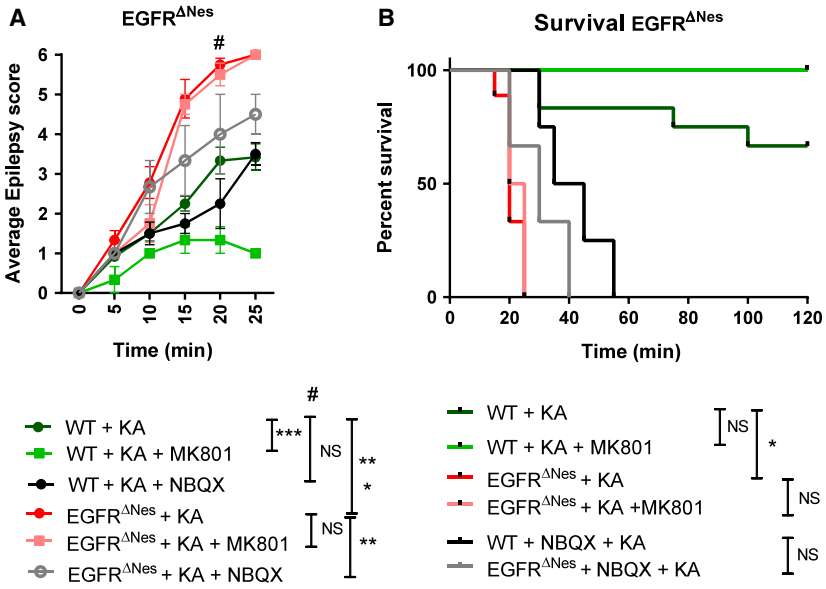

Fig. 9. The absence of EGFR in brain cells increases susceptibility to Kainic acid-induced epilepsy. (A) Treatment of EGFR$^{\Delta Nes}$ mice with Kainic Acid (KA) resulted in significantly more severe epileptic seizures than controls, which were not ameliorated with the NMDAR antagonist MK801 or the AMPAR antagonist NBQX. (B) Treatment with KA resulted in fatalities that were not rescued with pretreatment of MK801 or NBQX. *N*-values: WT + KA (12), WT + KA + MK801 (3), WT + KA + NBQX (4), EGFR$^{\Delta Nes}$+KA (9), EGFR$^{\Delta Nes}$+KA + MK801 (4), EGFR$^{\Delta Nes}$+KA + NBQX (3). Error bars indicate SEM; * indicates $P < 0.05$, ** $P < 0.005$, *** $P < 0.0005$. Statistical tests: A, *t*-test; B, Log-rank (Mantel–Cox) test.

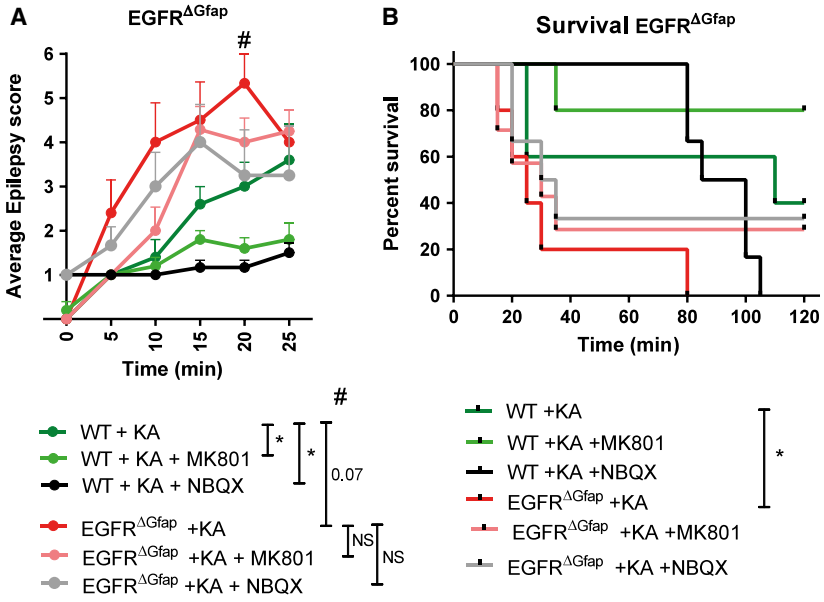

Fig. 10. EGFR$^{\Delta Gfap}$ mice display increased susceptibility to Kainic acid-induced epilepsy and not ameliorated by glutamate receptor antagonists. (A) Treatment of EGFR$^{\Delta Gfap}$ mice and control littermates with Kainic Acid (KA) resulted in severe epileptic seizures, which were not ameliorated with the NMDAR antagonist MK801 or the AMPAR antagonist NBQX. (B) Treatment of EGFR$^{\Delta Gfap}$ mice with KA resulted in fatalities that were not rescued with pretreatment of MK801 or NBQX. *N*-values: WT + KA (5), WT + KA + MK801 (5), WT + KA + NBQX (6), EGFR$^{\Delta Gfap}$+KA (5), EGFR$^{\Delta NGfap}$+KA+MK801 (7), EGFR$^{\Delta Gfap}$+KA + NBQX (6). Error bars indicate SEM; * indicates $P < 0.05$, ** $P < 0.005$, *** $P < 0.0005$. Statistical tests: A, *t*-test; B, Log-rank (Mantel–Cox) test.

seizure score 4, $P = 0.433$, $n = 4$). Pretreatment with MK801 also increased survival in Nestin and Gfap littermate control mice (0/3 deaths and 1/4 deaths, respectively) but had no effect on EGFR$^{\Delta Nes}$ survival following KA-induced epilepsy (4/4 deaths; Fig. 9B). In addition to NMDAR antagonism, pretreatment of Nestin littermate control mice with the AMPAR antagonist NBQX significantly reduced epileptic scores in control mice (15 min time point, median score 2, $P = 0.02$; $n = 4$; Fig. 9A) and significantly ameliorated KA-induced death (4/4 deaths, $P = 0.0013$; Fig. 9B). EGFR$^{\Delta Nes}$ KA-induced seizures were similarly significantly ameliorated following NBQX pretreatment (median score 3, $P = 0.02$; $n = 3$; Fig. 9A) but survival was not significantly affected (3/3 deaths, $P = 0.051$; Fig. 9B).

Similar to Nestin littermate control mice, pretreatment of Gfap littermate control mice with NBQX ($n = 6$; $P = 0.007$) or MK801 ($n = 5$; $P = 0.048$) significantly ameliorated seizures (Fig. 10A) but had little effect on survival (Fig. 10B). Pretreatment of EGFR$^{\Delta Gfap}$ mice with receptor antagonists ($n = 7$ MK801; $n = 6$ NBQX) had no significant effect on seizure severity or mouse survival following KA-induced epilepsy (Fig. 10A,B). These results demonstrate that EGFR$^{\Delta Nes}$ and EGFR$^{\Delta Gfap}$ mice are much more sensitive to KA treatment than controls, with EGFR$^{\Delta Nes}$ mice displaying a more aggressive epileptic response compared with EGFR$^{\Delta Gfap}$ mice.

EGFR$^{-/-}$ cortical-derived astrocytes show defective glutamate uptake *in vitro*

Next, we investigated the possible mechanism responsible for the hypersensitivity to KA-induced epileptic seizures in mice lacking the EGFR in the brain. KA leads to release of the excitatory neurotransmitter glutamate, which can directly stimulate glutamate receptors such as NMDAR1 and AMPAR1. The levels of glutamate are mainly regulated by glutamate transporters, which are abundantly expressed on astrocytes, whose primary function (among others) is to regulate extracellular glutamate levels. It has been shown that defective glutamate uptake by astrocytes can lead to neuronal death and degeneration (reviewed in [45]). Thus, increased expression of glutamate receptors and/or reduced expression of transporters could account for increased KA sensitivity. Glt1 and Glast are the two most prominent glutamate transporters in the adult brain accounting for the majority of glutamate transport activity in the forebrain and cerebellum, respectively [22,23,46]. As reported above, brains from young EGFR$^{\Delta}$ mice retain EGFR protein expression. Freshly isolated cortical astrocytes similarly identified

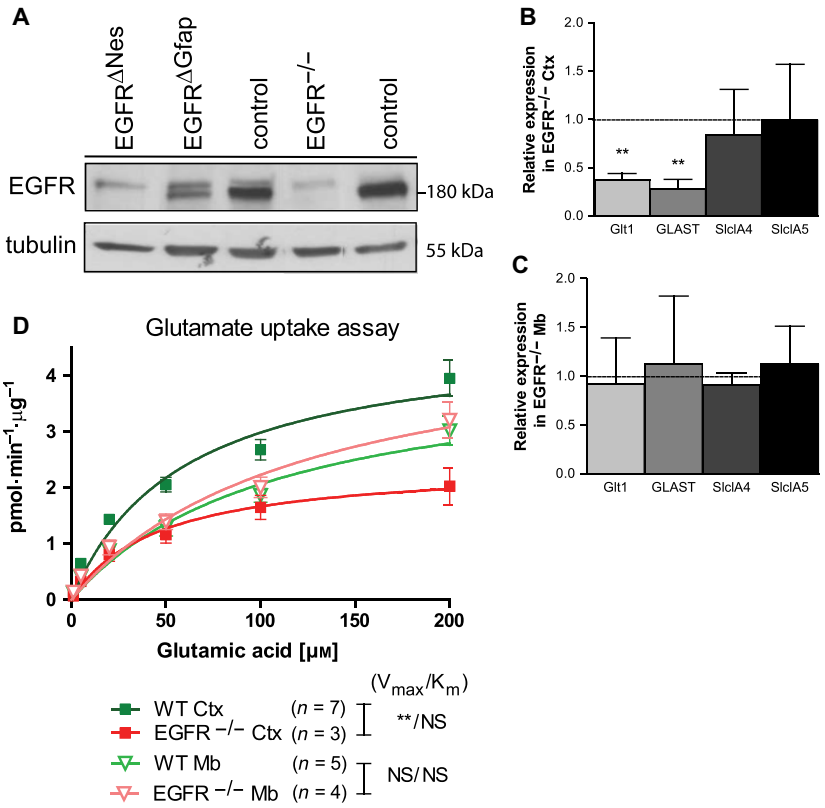

Fig. 11. EGFR$^{-/-}$ cortical astrocytes have deficient glutamate uptake capacity. (A) Western blot analysis of EGFR levels in cultured cortical astrocytes; EGFR protein bottom band. (B, C) Quantitative PCR analyses of EGFR$^{-/-}$ and control astrocytes derived from the neocortex (B; $n = 4$) and midbrain (C; $n = 4$). Astrocytes were assayed for *Glt1* (*Slc1A2*), *Glast* (*Slc1A3*), *Sl1c1A4,* and *Slc1A5* and normalized to *Gapdh*. (D) Glutamate uptake assay of isolated astrocytes normalized to assayed protein levels identified a significant glutamate uptake potential in EGFR$^{-/-}$ cortical but not midbrain-derived astrocytes. Significant values shown in order V_{max} then K_M. *N*-values: WT Ctx (7), EGFR$^{-/-}$ Ctx (3), WT Mb (5), EGFR$^{-/-}$ Mb (4). Error bars indicate SEM; $^{**}P < 0.005$; NS, not significant. Statistical tests: B/C, *t*-test; D, unpaired *t*-test with Welches correction.

protein expression, however, no protein was detected in EGFR$^{-/-}$ astrocytes (Fig. 11A). We, therefore, utilized EGFR$^{-/-}$ cortical and midbrain-derived astrocytes in subsequent glutamate transporter analyses.

To determine if cortical and/or midbrain-derived astrocytes from EGFR$^{-/-}$ mice had decreased expression of glutamate transporters we investigated mRNA isolated from cultured astrocytes ($n = 4$). We identified significantly reduced expression of *Glt1* (*Slc1a2*; $P = 0.0058$) and *Glast* (*Slc1a3*; $P = 0.001$) transcripts in EGFR$^{-/-}$ cortical-derived astrocytes but not in EGFR$^{-/-}$ midbrain-derived astrocytes compared with controls (Fig. 11B,C). No differences in *Slc1A4* or *Slc1A5* transcripts were observed between groups. These data indicate that EGFR is regulating the expression of glutamate transporter transcripts in cortical astrocytes but not in the midbrain.

To investigate the hypothesis that astrocytes in EGFR ablated brains have defective/reduced glutamate uptake we utilized the well-established glutamate uptake assay [47,48]. Primary cortical or midbrain astrocytes from P2 EGFR$^{-/-}$ mice or littermate controls were seeded into 24-well plates and incubated with tritium-labeled glutamate for 10 min under controlled conditions. We found that the total uptake capacity (V_{max}) of glutamate transporters was significantly reduced in cortical astrocytes (EGFR$^{-/-}$ V_{max} 2.429 pmol·min^{-1}·μg^{-1} ($n = 3$); control astrocytes V_{max} 4.740 pmol·min^{-1}·μg^{-1} ($n = 7$); $P = 0.001$), but not midbrain astrocytes (EGFR$^{-/-}$ V_{max} 4.978 pmol·min^{-1}·μg^{-1} ($n = 4$); control astrocytes V_{max} 4.316 pmol·min^{-1}·μg^{-1} ($n = 5$); $P = 0.679$) when normalized to total protein (Fig. 11D). However, the uptake function itself was not affected since the concentration of the half-maximal transport velocity (K_M) were similar for all populations (EGFR$^{-/-}$ cortical astrocytes, K_M 45.84 μM; control cortical astrocytes, K_M 58.96 μM, $P = 0.608$; EGFR$^{-/-}$ midbrain astrocytes, K_M 123.3 μM; control midbrain astrocytes, K_M 109.3 μM, $P = 0.4982$; Fig. 11D). These results indicate that cortical but not midbrain-derived astrocytes have significantly lower glutamate transporter expression. Astrocytes from EGFR-deficient mice are unable to efficiently transport the excitatory glutamate out of the synapse providing strong evidence that the observed neurodegeneration may be occurring due to excitotoxicity from excess glutamate.

Discussion

The objective of this study was to clarify the function of EGFR in the brain by employing EGFR knock-out (−/−) mice and mice lacking the EGFR specifically in

the brain by two different Cre lines (Nestin-Cre and GFAP-Cre). $EGFR^{-/-}$ mice present with an aggressive neurodegeneration shortly after birth. To determine if the neurodegeneration was associated with defective neural stem cell regulation we investigated the effect total loss of EGFR has on SVZ-derived stem/progenitor cell division in $EGFR^{-/-}$ mice. Utilizing *in vitro* neurosphere assays we showed that $EGFR^{-/-}$ neurospheres did not show the cardinal stem cell traits of self-renewal (symmetric stem cell division) or full differentiation capability illustrating that EGFR signaling is critical for these processes. These findings support previously published results that EGF and FGF growth factors are important for neural stem cell proliferation [28,30] but report for the first time the effect complete loss of EGFR has on the neurogenic niche *in vivo* in postnatal mice. Previous studies have reported the importance of EGFR expression during neural stem cell division with differential EGFR distribution to daughter cells resulting in progenitors with different proliferative, migratory, and differentiation responses to EGFR ligands [7]. Here, we show that with complete ablation of EGFR, cells derived from the SVZ show preferentially a glial-progenitor identity, suggesting that EGFR signaling plays an important role in the switch from neural stem cell to glial progenitors.

Due to the early mortality observed in $EGFR^{-/-}$ mice we could not utilize this model to investigate the effect EGFR loss has on neuron and astrocyte development. To this end we utlized the $EGFR^{\Delta Gfap}$ and $EGFR^{\Delta Nes}$ murine models. At birth, $EGFR^{\Delta}$ mice were indistinguishable from their littermates and were born at the expected Mendelian frequencies. Starting around weaning age both $EGFR^{\Delta}$ mice were consistently 20% smaller. Growth retardation was also observed in $EGFR^{-/-}$ mice [12,14,15] and in mice carrying knock-in of the human EGFR allele ($EGFR^{KI}$) [17], whose growth retardations have been attributed to premature chondrocyte differentiation [17]. However, this is unlikely to occur in $EGFR^{\Delta}$ mice where the EGFR was absent only in neural cells. Interestingly, mice lacking the EGFR family member ErbB2 in neural precursors ($ErbB2^{flox/flox}$; Nestin-Cre) are also growth retarded [49]. Here, the growth retardation seems to be a secondary effect of a disease affecting intestinal function, which occurs as a consequence of postnatal degeneration of enteric neurons due to reduced release of growth factors by enteric glia. However, the growth retardation in $ErbB2^{flox/flox}$; Nestin-Cre is more severe with mice dying before 8 weeks of age [49]. It is possible that enteric neurons are less affected by the absence of the EGFR. Alternatively the growth retardation observed in $EGFR^{\Delta}$ mice may be a direct consequence of the absence of EGFR signaling in the brain. Members of the EGFR family have been implicated in several functions in the hypothalamus, including locomotor activity [50]. ErbB4 signaling in hypothalamic astrocytes is linked to LHRH release and delayed female sexual maturation [51]. It is possible that the absence of the EGFR in hypothalamic cells may affect metabolism, leading to reduced feeding behavior or growth hormone secretion and may consequently be directly responsible for the growth retardation of $EGFR^{\Delta}$ mice. Despite their reduced size, mice lacking EGFR in the brain showed no significant changes in behavioral responses over control mice following a plethora of behavioral tests. Increased entries were recorded for $EGFR^{\Delta}$ mice in the elevated plus maze test illustrating a possible increased anxiety in these mice. This anxiety may be attributed to the loss of EGFR as it has been shown that antagonism of EGFR in cancer patients has caused increased anxiety and depression [52]. However, these symptoms could also be attributable to the severe skin rash caused by EGFR inhibition [53] and remains inconclusive as to whether mice experience like-minded states of anxiety.

Initially, we had planned to use the conditional knock-out strategy to analyze in which neural cell-type EGFR signaling is required to prevent the cortical degeneration. However, no $EGFR^{\Delta Gfap}$ mice and only a small percentage of $EGFR^{\Delta Nes}$ mice showed signs of cortical degeneration throughout their lifespan. Extensive analysis with several neuronal markers did not reveal abnormal neuronal layering of cortical layers in EGFR-deficient brains. One phenotype observed in the brain of $EGFR^{-/-}$ mice also found in $EGFR^{\Delta}$ brains are the ectopic neurons in the white matter of the hippocampus. The presence of these ectopic neurons indicates a function for the EGFR in neuronal migration. EGFR signaling has previously been implicated in mediating migratory processes in the brain [3,54]. The EGFR family member ErbB4 is responsible for guiding the migration of a subset of inhibitory interneurons from the subpallium to the cortex and the hippocampus [55]. In the hippocampus, interneuron migration occurs along prospective white matter tracts [56] and during early postnatal development EGFR expression was observed along these migratory routes [57]. Interestingly, the ectopic neurons found in $EGFR^{\Delta}$ mice are situated along this route. HB-EGF is highly expressed in the hippocampus during late embryonic development [58]. Therefore, it is possible that HB-EGF-induced EGFR signaling contributes to the migration of interneurons into the hippocampus.

Due to the high expression levels of HB-EGF the EGFR protein is probably degraded earlier in the hippocampus than in the cortex, and the absence of EGFR signaling during later stages of migration leads to the ectopic arrest of neurons in the white matter tract.

To analyze the function of the EGFR in the adult brain we applied several models of brain injury. These experiments were performed in adult mice where the EGFR protein could no longer be detected in the brain. In models where the major response to insults is reactive astrogliosis, like stab wounding and Prion infection, we did not observe any defects in mice lacking the EGFR in the brain. These results suggest that although EGFR signaling may play a supportive role during astrogliosis it is not strictly required for injury repair. The third model of brain injury applied was the KA seizure model. Susceptibility to Kainic Acid-induced toxicity has been described to differ in intensity according to the genetic background [41], which might explain the different sensitivities of the Nes and Gfap control mice. Independent of the genetic background, $EGFR^{\Delta Gfap}$ and $EGFR^{\Delta Nes}$ mice were clearly more susceptible to KA-induced seizures, with more severe and prolonged seizures most often leading to fatality. The excitatory mechanism occurring in an epileptic seizure has been well clarified to be caused by activation of the ionotropic glutamate receptors NMDAR, AMPAR, and the Kainate receptor [59] (reviewed extensively in [60]). Complementary studies have shown that successful inhibition of ionotropic NMDAR [61,62] and AMPAR [63] have significantly ameliorated epileptic seizures. Indeed treatment with the AMPAR and NMDAR antagonists MK801 and NBQX significantly ameliorated the KA-induced seizures in control mice. These antagonists had, however, no effect on seizures or survival in $EGFR^{\Delta Gfap}$ and $EGFR^{\Delta Nes}$ mice. The reason for this might be the short half-life of these antagonists combined with the excess glutamate present in EGFR deficient brains. The increased excitotoxicity observed in mice lacking the EGFR in the brain may be the result of diminished glutamate uptake by astrocytes, which express reduced levels of the glutamate transporters Glt1 and Glast. [19,64–66]. Glt1 and Glast have been well documented to play a critical role in regulating the amount of glutamate in the synaptic cleft between pre- and postsynaptic neurons [22,23,46,67–70]. Furthermore, EGFR has been implicated in the regulation of astrocytic glutamate transporters *in vitro* and specifically, it has been shown that Glt1 expression is positively regulated by EGFR activity in cultured astrocytes [67,68]. Interestingly, we found that loss of EGFR affected the expression of *Glt1* and *Glast* exclusively in cortical-derived astrocytes but not in midbrain-derived astrocytes. Similarly, glutamate uptake was reduced in cortical but not midbrain derived $EGFR^{-/-}$ astrocytes. In conjunction with our findings, studies reporting that transgenic animals overexpressing *Glt1* were less sensitive to seizure-induced neuronal damage illustrate that amelioration of seizures is at least in part attributed to the functional activity of Glt1 [68]. It remains unknown as to why midbrain astrocytes are unaffected by the loss of EGFR. One explanation is the absence of a postnatal neurogenic niche, or conversely, the cortex phenotype may be associated with the presence of a neurogenic niche [27,71], however, further studies are require to elucidate these hypotheses.

In summary, we demonstrate that complete loss of EGFR in the brain results in severe neurodegeneration and a reduction in the neurogenic potential of neural stem cells. In contrast, Cre-mediated deletion of EGFR in the brain results in only rare neurodegeneration but severe susceptibility to KA induced epilepsy that is not ameliorated with glutamate receptor antagonists. We show that cortical but not midbrain-derived astrocytes have reduced glutamate transporter expression and reduced glutamate transporter activity providing a mechanism of glutamate excitotoxic-induced neuronal death. Elucidating the mechanism by which EGFR prevents glutamate-mediated neuronal toxicity may have important implications in identifying treatment options for neurodegenerative and seizure-associated diseases in the brain.

Material and methods

Animal experiments

The $EGFR^{f/f}$ mice bred to GFAP-Cre+ and Nestin-Cre+ mice were maintained on a mixed genetic background (C57BL/6J × 129/Sv × CBA/J). $EGFR^{-/-}$ mice were of pure outbred MF1 genetic background. In all experiments EGFR expressing littermates ($EGFR^{f/f}$ or *Cre+* or $EGFR^{+/+}$) served as controls to the respective EGFR deleted mice. Because of the high stability of the EGFR protein, breedings were set up to generate mice harboring always a complete knock-out allele together with a floxed allele ($EGFR^{f/-}$). In this way, mice lacking EGFR protein in the brain ($EGFR^{\Delta Gfap}$ and $EGFR^{\Delta Nes}$ mice.) could be more efficiently generated after breeding to Nes-Cre or GFAP-Cre mice. Genotyping was performed by PCR as previously described [19,72]. Primer sequences can be obtained upon request. Mice were housed in a 12-h dark/light cycle with water and food *ad libitum* and kept/bred in the animal facility of the Medical University of Vienna in

accordance with institutional policies and federal guidelines. Animal experiments were approved by the Animal Experimental Ethics Committee of the Medical University of Vienna and the Austrian Federal Ministry of Science and Research. (Animal license numbers: GZ 66.009/124-BrGT/2003; GZ 66.009/109-BrGT/2003; BMWF-66.009/0073-II/10b/2010 BMWF-66.009/0074-II/10b/2010; BMWFW-66.009/0200-WF/II/3b/2014; and BMWFW-66.009/0199-WF/II/3b/2014).

Behavioral tests

Animals were initially assessed by Basic Observational Neurological and physical assessment (NOB) as detailed in [73]. Mice were then assayed for a number of behavioral tests including the Rota rod test (RR) [74], Open field test (OFT) [75], Light Dark Box test (LDB) [76], Elevated Plus Maze (EPM) [77], Tail suspension test (TST) [78], Forced Swim test (FST) [79], and sucrose Preference test (SPT) [80,81]. Tests were performed as detailed by references linked above. Data were recorded as percentage/number of entries (EPM, LDB, OFT), percentage/length of time spent (EPM, RR, LDB, OFT), percentage/length of distance travelled (EPM, LDB, OFT), percent sucrose (SPT), and percent immobility (FST, TST). Results analyzed with one-way ANOVA with *post hoc* Scheffe tests.

Southern blot

Southern blots were carried out as previously described [31] with some changes: Mouse genomic DNA was digested overnight. The samples were run on a 0.7% agarose gel and blotted overnight. Probes were labeled using the Stratagene labeling kit II (Amersham, Buckinghamshire, England) and hybridization was performed in Church Buffer at 65 °C overnight. Membranes were wrapped in Saran Wrap and films were exposed for several days.

Western blot

Cells/tissues were homogenized with ice-cold solubilization buffer (50 mM Hepes pH7.3, 150 mM NaCl, 10% glycerol, 1.5 mM $MgCl_2$, 1% Triton X-100, 1 mM EGTA pH8, 10 mM $Na_2P_2O_7$, 0.001% Aprotinin, 0.001% Leupeptin, 25 mM NaF, 1 mM $NaVO_3$, 1 mM PMSF, 20 mM PNPP, 10 mM sodiumpyrophosphate) and lyzed on ice for 30 min. Lysates were cleared by centrifugation for 10 min at 10 000 ***g*** and 4 °C. Lysates were shock frozen and stored at −80 °C. Protein separation was performed on SDS/PAGE Gels and proteins were transferred to nitrocellulose membranes (Amersham). Membranes were incubated with primary antibodies overnight and with secondary antibodies for an hour. Detection was performed using ECL (Amersham). Antibodies used in western blot: anti-EGFR (Upstate 06–129, 1 : 1000), anti-actin (Sigma, 1 : 100, St. Louis, Missouri, United States), anti-tubulin (Sigma, 1 : 100), anti-Rabbit HRP (DA(−/−, 1 : 10 000), anti-Sheep HRP (DA(−/− 1 : 10 000).

Astrocyte cultures and qPCR

Astrocytes were prepared between E18.5 and P2. Single-cell suspensions were seeded in astrocyte medium (DMEM high glucose; 2 mM glutamine; 1 × penicillin/streptomycin; 5% fetal bovine serum (FBS); 5% Horse Serum (HS). Nearly confluent astrocyte cultures were trypsinized and reseeded in astrocyte medium. DMEM high glucose, penicillin/streptomycin, horse serum, and glutamine were obtained from Invitrogen and FBS was purchased from PAA. RNA was isolated using a QIAgen spin miniprep kit (27104) and cDNA obtained from total RNA by reverse transcription with SUPERSCRIPT First-Strand Synthesis System (Invitrogen, Carlsbad, California, United States). qPCR analysis was done as described in [19]. Assay on demand Taqman probes from Applied Biosystems (Foster City, California, United States): Glt1: Mm00441457_m1; GLAST: Mm00600697_m1; Slc1A4: Mm00444532_m1; Slc1A5: Mm00436603_m1.

Neurosphere assays

Neurospheres were isolated as detailed in [27]. Briefly, SVZ-derived tissue was dissociated in 1 × Accutase (Life Technologies A1110501, Carlsbad, California, United States) for 7 min at 37 °C, cells centrifuged at 100 ***g*** for 5 min, supernatant removed and cells resuspended in 2 mL NS media (DMEM Thermo, 50-124-PA, Waltham, Massachusetts, United States; F12, Gibco 21700-026, Waltham, Massachusetts, United States; Penicillin/Streptomycin, Gibco 15140-122; NaHCO3, Sigma S5761; Glucose, Sigma G7021; HEPES, Sigma H4034) supplemented with 4 mL 10% BSA solution, 2 mL Penicilin/Streptomycin and 20 mL Neurocult proliferation supplement (mouse, Stem Cell Technologies 05701, Vancouver, Canada), and then filtered through a 40-μm mesh (BD falcon 352340). Neurospheres were cultured with 20 $ng{\cdot}mL^{-1}$ EGF (Sigma E4127, St. Louis, Missouri, United States) and/or 10 $ng{\cdot}mL^{-1}$ bFGF (Preprotech 100-18B, Rocky Hill, Connecticut, United States). For differentiation assays, neurospheres at passage 5 were seeded into 24 well plates with 10% FBS and growth factors removed. Following 6 days cells were fixed with 4% paraformaldehyde and stained via immunofluorescent methods. GFAP antibody (DAKO Z0334, Agilent Technologies, Vienna, Austria), Tuj1 antibody (Promega; G712A, Madison, Wisconsin, United States).

Stabwound/blood–brain barrier HRP experiments

The animals were anesthetized with a combination of ketamine and xylazine according to standard protocols.

Forebrain stab injuries were inflicted using a sterile No.11 scalpel blade 1 mm rostral to the bregma into the right hemisphere. The skin above the wound was closed with a suture clip. Mice were killed 7 and 35 days after the stab wounding using a lethal dose of ketamine and xylazine and were transcardially perfused with 4% paraformaldehyde (PFA). Whole mouse brains were fixed in 4% PFA, and then incubated in 20% sucrose overnight. After embedding in OCT (Sakura, Alphen aan den Rijn, The Netherlands) the tissue was shock frozen on dry ice and stored at −80 °C. For the BBB experiment HRP (5 mg/mouse) was injected with into the tail vein as detailed in [82]. One hour after the HRP injection mice were killed and the brains were prepared as described for the stabwound experiment.

Kainic acid-induced epilepsy

Mice were intraperitoneally injected with Kainic Acid at a dose of 25 $mg{\cdot}kg^{-1}$. Mice were observed for 120 min following treatment, and kainate scores were evaluated every 5 min on a scale from 0 to 6. Seizures were scored as follows: 1, arrest of motion; 2, appearance of rigid posture; 3, myoclonic jerks of head and neck, with brief twitching movements; 4, forelimb clonus and partial rearing, unilateral; 5, forelimb clonus, rearing, falling, bilateral; 6, generalized tonic–clonic activity with loss of postural tone, often resulting in death. To study NMDAR and AMPAR antagonism we used MK801 (Tocris 0924, Bristol, United Kingdom) and NBQX (Tocris 1044), respectively. MK801 was administered 20 min prior to KA injection at a concentration of 0.2 $\mu g{\cdot}g^{-1}$ and NBQX was injected 10 min prior to KA injection at 30 $\mu g{\cdot}g^{-1}$ concentrations. All injections were done via intraperitoneal injection. Given the half-lives of the antagonists also used in this study we underwent analysis at 20 min post-KA injection.

Prion infection

Mice were intracerebrally injected with the RML prion strain at doses of 10^{-1}U LD50 and 10^{-4}U LD50. Mice either succumbed to the disease or were euthanized when pathological symptoms became apparent. Brains were then fixed in PFA and processed for histology as described [37].

Histology and immunohistochemistry

For routine histology brain sections were stained with hematoxylin/eosin and Bielschowsky silver stain according to standard protocols. Immunohistochemical stainings were carried out on an automated Nexus staining apparatus, following the manufacturer's guidelines. Visualization was achieved using biotin/avidin-peroxidase (DAKO K3954) and diaminobenzidine as a chromogen. For the BBB experiment transverse brain sections were developed using DAB (diaminobenzidinetetrahydrochlorid) as HRP substrate. Sections were rinsed in PBS and stained with DAB for 20 min. Stainings were visualized using the DAB peroxidase substrate kit (Vectashield, Burlingame, California, United States), rinsed 3 × with PBS and mounted onto slides. After dehydration sections were coverslipped. For Immunofluorescent imaging, stainings were performed on 5uM cryosectioned tissue following standard protocols and if necessary a citric acid buffer antigen retrieval protocol was applied. Antibodies used: F4/80 (eBioscience 14-4801, Thermofisher), anti-GFAP (1 : 300, DAKO Z0334), NeuN (Millipore MAB377, Burlington, Massachusetts, United States). Fixation and staining of the brains used in the prion experiment was performed as described [37].

Glutamate uptake assays

Glutamate uptake assays were carried out on $EGFR^{+/+}$ or $EGFR^{-/-}$ cortical and midbrain derived astrocytes as detailed in [72]. Briefly, primary isolated astrocytes were seeded into 24-well plates at a density of 50 000 cells/well prior to carrying out the uptake assay. Following approximately 3 days in culture (or ~ 80% confluence. Minimum 70% confluence) uptake assays were performed. Briefly, cells were washed with Krebs-HEPES buffer (KHB: 10 mM HEPES, 130 mM NaCl, 1.3 mM KH2PO4, 1.5 mM CaCl2, 0.5 mM MgSO4, pH 7.4 adjusted with NaOH). After a 15 min preincubation step in KHB, glutamate uptake was started by adding KHB containing 0.05 μM [^{3}H] glutamate (Perkin Elmer, Waltham, Massachusetts, United States; specific activity: 50.6 Ci/mmol) including different concentrations of unlabeled glutamate (up to 200 μM) to the cultures. Uptake was done at room temperature and stopped after 10 min by adding ice-cold KHB. Nonspecific uptake was performed in the presence of 10 μM L-trans-pyrrolidine-2,4-dicarboxylate (PDC). Cells were washed twice with ice-cold buffer prior to cell lysis. Radioactivity was measured using a liquid scintillation counter and 30% of the cell lysate was used for protein determination using a bicinchoninic acid assay (Bio-Rad, Hercules, California, United States).

Statistical analysis

Statistical analysis and graphical representation were performed using Microsoft Excel and Graph Pad Prism Software. Experiments were analyzed using t-tests, one-way ANOVA followed by *post hoc* Scheffe tests (for behavioral analyses), Cox–Mantel tests (for survival plots) and a P-value < 0.05 was considered statistically significant. All n-values shown indicate biological repeats.

Acknowledgments

We are grateful to Martina Hammer for maintaining our mouse colonies and help with *in vivo* mouse procedures. We thank Alexandra Bogusch, Gertraud

Steniczka, and Sarah Bardakji for excellent technical assistance and help with genotyping. We are thankful to Renate Kroismayr for RNA analysis of glutamate transporters. We thank Michael Freissmuth and Claudia Petritsch for critical discussions and comments on the manuscript. BW was recipient of a DOC-Fellowship of the Austrian Academy of Sciences (ÖAW). This work was supported by the Austrian Science Fund (FWF) grants P18421, DK W1212, and SFB F3518-B20 (to MS), F3503-B20 and DK W1232 (to HHS) and F3516-B20 (to DDP) and the Austrian Federal Government's GEN-AU program 'Austromouse' (GZ 200.147/1-VI/1a/2006 and 820966).

Conflict of interest

The authors declare that they have no conflict of interest.

Author contributions

BW and JR conceived and designed the experiments, and performed most of them. JR wrote, edited, and submitted the manuscript. EG performed the FACS analyses. TS and HHS helped with the glutamate uptake assays and participated in the interpretation of the data; HHS provided the requested funding for this project part; DK and DDP performed the behavioral studies; and FH performed the stab wound and prion infection experiments. MS conceived, designed, and supervised the whole project and provided the requested funding.

References

1 Sibilia M, Kroismayr R, Lichtenberger BM, Natarajan A, Hecking M & Holcmann M (2007) The epidermal growth factor receptor: from development to tumorigenesis. *Differentiation* **75**, 770–787.
2 Yarden Y & Sliwkowski MX (2001) Untangling the ErbB signalling network. *Nat Rev Mol Cell Biol* **2**, 127–137.
3 Caric D, Raphael H, Viti J, Feathers A, Wancio D & Lillien L (2001) EGFRs mediate chemotactic migration in the developing telencephalon. *Development* **128**, 4203–4216.
4 Kornblum HI, Hussain RJ, Bronstein JM, Gall CM, Lee DC & Seroogy KB (1997) Prenatal ontogeny of the epidermal growth factor receptor and its ligand, transforming growth factor alpha, in the rat brain. *J Comp Neurol* **380**, 243–261.
5 Lillien L & Raphael H (2000) BMP and FGF regulate the development of EGF-responsive neural progenitor cells. *Development* **127**, 4993–5005.
6 Viti J, Feathers A, Phillips J & Lillien L (2003) Epidermal growth factor receptors control competence to interpret leukemia inhibitory factor as an astrocyte inducer in developing cortex. *J Neurosci* **23**, 3385–3393.
7 Sun Y, Goderie SK & Temple S (2005) Asymmetric distribution of EGFR receptor during mitosis generates diverse CNS progenitor cells. *Neuron* **45**, 873–886.
8 Doetsch F (2003) The glial identity of neural stem cells. *Nat Neurosci* **6**, 1127–1134.
9 Pastrana E, Cheng LC & Doetsch F (2009) Simultaneous prospective purification of adult subventricular zone neural stem cells and their progeny. *Proc Natl Acad Sci USA* **106**, 6387–6392.
10 Codega P, Silva-Vargas V, Paul A, Maldonado-Soto AR, Deleo AM, Pastrana E & Doetsch F (2014) Prospective identification and purification of quiescent adult neural stem cells from their *in vivo* niche. *Neuron* **82**, 545–559.
11 Aguirre A, Rubio ME & Gallo V (2010) Notch and EGFR pathway interaction regulates neural stem cell number and self-renewal. *Nature* **467**, 323–327.
12 Miettinen PJ, Berger JE, Meneses J, Phung Y, Pedersen RA, Werb Z & Derynck R (1995) Epithelial immaturity and multiorgan failure in mice lacking epidermal growth factor receptor. *Nature* **376**, 337–341.
13 Sibilia M, Steinbach JP, Stingl L, Aguzzi A & Wagner EF (1998) A strain-independent postnatal neurodegeneration in mice lacking the EGF receptor. *EMBO J* **17**, 719–731.
14 Sibilia M & Wagner EF (1995) Strain-dependent epithelial defects in mice lacking the EGF receptor. *Science* **269**, 234–238.
15 Threadgill DW, Dlugosz AA, Hansen LA, Tennenbaum T, Lichti U, Yee D, LaMantia C, Mourton T, Herrup K, Harris RC *et al.* (1995) Targeted disruption of mouse EGF receptor: effect of genetic background on mutant phenotype. *Science* **269**, 230–234.
16 Miettinen PJ, Chin JR, Shum L, Slavkin HC, Shuler CF, Derynck R & Werb Z (1999) Epidermal growth factor receptor function is necessary for normal craniofacial development and palate closure. *Nat Genet* **22**, 69–73.
17 Sibilia M, Wagner B, Hoebertz A, Elliott C, Marino S, Jochum W & Wagner EF (2003) Mice humanised for the EGF receptor display hypomorphic phenotypes in skin, bone and heart. *Development* **130**, 4515–4525.
18 Kornblum HI, Hussain R, Wiesen J, Miettinen P, Zurcher SD, Chow K, Derynck R & Werb Z (1998) Abnormal astrocyte development and neuronal death in mice lacking the epidermal growth factor receptor. *J Neurosci Res* **53**, 697–717.
19 Wagner B, Natarajan A, Grunaug S, Kroismayr R, Wagner EF & Sibilia M (2006) Neuronal survival

depends on EGFR signaling in cortical but not midbrain astrocytes. *EMBO J* **25**, 752–762.
20 Wetherington J, Serrano G & Dingledine R (2008) Astrocytes in the epileptic brain. *Neuron* **58**, 168–178.
21 Lehre KP, Levy LM, Ottersen OP, Storm-Mathisen J & Danbolt NC (1995) Differential expression of two glial glutamate transporters in the rat brain: quantitative and immunocytochemical observations. *J Neurosci* **15**, 1835–1853.
22 Rothstein JD, Martin L, Levey AI, Dykes-Hoberg M, Jin L, Wu D, Nash N & Kuncl RW (1994) Localization of neuronal and glial glutamate transporters. *Neuron* **13**, 713–725.
23 Rothstein JD, Dykes-Hoberg M, Pardo CA, Bristol LA, Jin L, Kuncl RW, Kanai Y, Hediger MA, Wang Y, Schielke JP *et al.* (1996) Knockout of glutamate transporters reveals a major role for astroglial transport in excitotoxicity and clearance of glutamate. *Neuron* **16**, 675–686.
24 Tanaka K, Watase K, Manabe T, Yamada K, Watanabe M, Takahashi K, Iwama H, Nishikawa T, Ichihara N, Kikuchi T *et al.* (1997) Epilepsy and exacerbation of brain injury in mice lacking the glutamate transporter GLT-1. *Science* **276**, 1699–1702.
25 Tronche F, Kellendonk C, Kretz O, Gass P, Anlag K, Orban PC, Bock R, Klein R & Schutz G (1999) Disruption of the glucocorticoid receptor gene in the nervous system results in reduced anxiety. *Nat Genet* **23**, 99–103.
26 Marino S, Vooijs M, van Der Gulden H, Jonkers J & Berns A (2000) Induction of medulloblastomas in p53-null mutant mice by somatic inactivation of Rb in the external granular layer cells of the cerebellum. *Genes Dev* **14**, 994–1004.
27 Reynolds BA & Weiss S (1992) Generation of neurons and astrocytes from isolated cells of the adult mammalian central nervous system. *Science* **255**, 1707–1710.
28 Reynolds BA & Weiss S (1996) Clonal and population analyses demonstrate that an EGF-responsive mammalian embryonic CNS precursor is a stem cell. *Dev Biol* **175**, 1–13.
29 Rietze RL & Reynolds BA (2006) Neural stem cell isolation and characterization. *Methods Enzymol* **419**, 3–23.
30 Tropepe V, Sibilia M, Ciruna BG, Rossant J, Wagner EF & van der Kooy D (1999) Distinct neural stem cells proliferate in response to EGF and FGF in the developing mouse telencephalon. *Dev Biol* **208**, 166–188.
31 Natarajan A, Wagner B & Sibilia M (2007) The EGF receptor is required for efficient liver regeneration. *Proc Natl Acad Sci USA* **104**, 17081–17086.
32 Janzer RC & Raff MC (1987) Astrocytes induce blood-brain barrier properties in endothelial cells. *Nature* **325**, 253–257.
33 Sofroniew MV & Vinters HV (2010) Astrocytes: biology and pathology. *Acta Neuropathol* **119**, 7–35.
34 Levison SW, Jiang FJ, Stoltzfus OK & Ducceschi MH (2000) IL-6-type cytokines enhance epidermal growth factor-stimulated astrocyte proliferation. *Glia* **32**, 328–337.
35 Rabchevsky AG, Weinitz JM, Coulpier M, Fages C, Tinel M & Junier MP (1998) A role for transforming growth factor alpha as an inducer of astrogliosis. *J Neurosci* **18**, 10541–10552.
36 Bush TG, Puvanachandra N, Horner CH, Polito A, Ostenfeld T, Svendsen CN, Mucke L, Johnson MH & Sofroniew MV (1999) Leukocyte infiltration, neuronal degeneration, and neurite outgrowth after ablation of scar-forming, reactive astrocytes in adult transgenic mice. *Neuron* **23**, 297–308.
37 Steele AD, Hutter G, Jackson WS, Heppner FL, Borkowski AW, King OD, Raymond GJ, Aguzzi A & Lindquist S (2008) Heat shock factor 1 regulates lifespan as distinct from disease onset in prion disease. *Proc Natl Acad Sci USA* **105**, 13626–13631.
38 Ben-Ari Y (1985) Limbic seizure and brain damage produced by kainic acid: mechanisms and relevance to human temporal lobe epilepsy. *Neuroscience* **14**, 375–403.
39 Ferkany JW, Zaczek R & Coyle JT (1984) The mechanism of kainic acid neurotoxicity. *Nature* **308**, 561–562.
40 Zhang XM & Zhu J (2011) Kainic Acid-induced neurotoxicity: targeting glial responses and glia-derived cytokines. *Curr Neuropharmacol* **9**, 388–398.
41 Zheng XY, Zhang HL, Luo Q & Zhu J (2011) Kainic acid-induced neurodegenerative model: potentials and limitations. *J Biomed Biotechnol* **2011**, 457079.
42 Behrens A, Sibilia M & Wagner EF (1999) Amino-terminal phosphorylation of c-Jun regulates stress-induced apoptosis and cellular proliferation. *Nat Genet* **21**, 326–329.
43 Yang DD, Kuan CY, Whitmarsh AJ, Rincon M, Zheng TS, Davis RJ, Rakic P & Flavell RA (1997) Absence of excitotoxicity-induced apoptosis in the hippocampus of mice lacking the Jnk3 gene. *Nature* **389**, 865–870.
44 Wu G, Lu ZH, Wang J, Wang Y, Xie X, Meyenhofer MF & Ledeen RW (2005) Enhanced susceptibility to kainate-induced seizures, neuronal apoptosis, and death in mice lacking gangliotetraose gangliosides: protection with LIGA 20, a membrane-permeant analog of GM1. *J Neurosci* **25**, 11014–11022.
45 Sanchez-Carbente MR & Massieu L (1999) Transient inhibition of glutamate uptake *in vivo* induces neurodegeneration when energy metabolism is impaired. *J Neurochem* **72**, 129–138.
46 Rothstein JD, Van Kammen M, Levey AI, Martin LJ & Kuncl RW (1995) Selective loss of glial glutamate transporter GLT-1 in amyotrophic lateral sclerosis. *Ann Neurol* **38**, 73–84.

47 Wadiche JI, Arriza JL, Amara SG & Kavanaugh MP (1995) Kinetics of a human glutamate transporter. *Neuron* **14**, 1019–1027.
48 Wadiche JI, Amara SG & Kavanaugh MP (1995) Ion fluxes associated with excitatory amino acid transport. *Neuron* **15**, 721–728.
49 Crone SA & Lee KF (2002) The bound leading the bound: target-derived receptors act as guidance cues. *Neuron* **36**, 333–335.
50 Kramer A, Yang FC, Snodgrass P, Li X, Scammell TE, Davis FC & Weitz CJ (2001) Regulation of daily locomotor activity and sleep by hypothalamic EGF receptor signaling. *Science* **294**, 2511–2515.
51 Prevot V, Rio C, Cho GJ, Lomniczi A, Heger S, Neville CM, Rosenthal NA, Ojeda SR & Corfas G (2003) Normal female sexual development requires neuregulin-erbB receptor signaling in hypothalamic astrocytes. *J Neurosci* **23**, 230–239.
52 Wagner LI & Lacouture ME (2007) Dermatologic toxicities associated with EGFR inhibitors: the clinical psychologist's perspective. Impact on health-related quality of life and implications for clinical management of psychological sequelae. *Oncology* **21**, 34–36.
53 Lichtenberger BM, Gerber PA, Holcmann M, Buhren BA, Amberg N, Smolle V, Schrumpf H, Boelke E, Ansari P, Mackenzie C *et al.* (2013) Epidermal EGFR controls cutaneous host defense and prevents inflammation. *Sci Transl Med* **5**, 199ra111.
54 Aguirre A, Rizvi TA, Ratner N & Gallo V (2005) Overexpression of the epidermal growth factor receptor confers migratory properties to nonmigratory postnatal neural progenitors. *J Neurosci* **25**, 11092–11106.
55 Flames N, Long JE, Garratt AN, Fischer TM, Gassmann M, Birchmeier C, Lai C, Rubenstein JL & Marin O (2004) Short- and long-range attraction of cortical GABAergic interneurons by neuregulin-1. *Neuron* **44**, 251–261.
56 Danglot L, Triller A & Marty S (2006) The development of hippocampal interneurons in rodents. *Hippocampus* **16**, 1032–1060.
57 Fox IJ & Kornblum HI (2005) Developmental profile of ErbB receptors in murine central nervous system: implications for functional interactions. *J Neurosci Res* **79**, 584–597.
58 Kornblum HI, Zurcher SD, Werb Z, Derynck R & Seroogy KB (1999) Multiple trophic actions of heparin-binding epidermal growth factor (HB-EGF) in the central nervous system. *Eur J Neuorsci* **11**, 3236–3246.
59 Cotman CW, Monaghan DT & Ganong AH (1988) Excitatory amino acid neurotransmission: NMDA receptors and Hebb-type synaptic plasticity. *Annu Rev Neurosci* **11**, 61–80.
60 Loscher W (1998) Pharmacology of glutamate receptor antagonists in the kindling model of epilepsy. *Prog Neurobiol* **54**, 721–741.
61 Stafstrom CE, Holmes GL & Thompson JL (1993) MK801 pretreatment reduces kainic acid-induced spontaneous seizures in prepubescent rats. *Epilepsy Res* **14**, 41–48.
62 Lai MC, Lui CC, Yang SN, Wang JY & Huang LT (2009) Epileptogenesis is increased in rats with neonatal isolation and early-life seizure and ameliorated by MK-801: a long-term MRI and histological study. *Pediatr Res* **66**, 441–447.
63 Namba T, Morimoto K, Sato K, Yamada N & Kuroda S (1994) Antiepileptogenic and anticonvulsant effects of NBQX, a selective AMPA receptor antagonist, in the rat kindling model of epilepsy. *Brain Res* **638**, 36–44.
64 Casper D, Mytilineou C & Blum M (1991) EGF enhances the survival of dopamine neurons in rat embryonic mesencephalon primary cell culture. *J Neurosci Res* **30**, 372–381.
65 Sibilia M, Fleischmann A, Behrens A, Stingl L, Carroll J, Watt FM, Schlessinger J & Wagner EF (2000) The EGF receptor provides an essential survival signal for SOS-dependent skin tumor development. *Cell* **102**, 211–220.
66 Yamada M, Enokido Y, Ikeuchi T & Hatanaka H (1995) Epidermal growth factor prevents oxygen-triggered apoptosis and induces sustained signalling in cultured rat cerebral cortical neurons. *Eur J Neuorsci* **7**, 2130–2138.
67 Li LB, Toan SV, Zelenaia O, Watson DJ, Wolfe JH, Rothstein JD & Robinson MB (2006) Regulation of astrocytic glutamate transporter expression by Akt: evidence for a selective transcriptional effect on the GLT-1/EAAT2 subtype. *J Neurochem* **97**, 759–771.
68 Zelenaia O, Schlag BD, Gochenauer GE, Ganel R, Song W, Beesley JS, Grinspan JB, Rothstein JD & Robinson MB (2000) Epidermal growth factor receptor agonists increase expression of glutamate transporter GLT-1 in astrocytes through pathways dependent on phosphatidylinositol 3-kinase and transcription factor NF-kappaB. *Mol Pharmacol* **57**, 667–678.
69 Karlsson RM, Tanaka K, Saksida LM, Bussey TJ, Heilig M & Holmes A (2009) Assessment of glutamate transporter GLAST (EAAT1)-deficient mice for phenotypes relevant to the negative and executive/cognitive symptoms of schizophrenia. *Neuropsychopharmacology* **34**, 1578–1589.
70 Watase K, Hashimoto K, Kano M, Yamada K, Watanabe M, Inoue Y, Okuyama S, Sakagawa T, Ogawa S, Kawashima N *et al.* (1998) Motor discoordination and increased susceptibility to cerebellar injury in GLAST mutant mice. *Eur J Neuorsci* **10**, 976–988.
71 Doetsch F, Caille I, Lim DA, Garcia-Verdugo JM & Alvarez-Buylla A (1999) Subventricular zone astrocytes are neural stem cells in the adult mammalian brain. *Cell* **97**, 703–716.

72 Lanaya H, Natarajan A, Komposch K, Li L, Amberg N, Chen L, Wculek SK, Hammer M, Zenz R, Peck-Radosavljevic M *et al.* (2014) EGFR has a tumour-promoting role in liver macrophages during hepatocellular carcinoma formation. *Nat Cell Biol* **16**, 972–987.
73 Irwin S (1968) Comprehensive observational assessment: Ia. A systematic, quantitative procedure for assessing the behavioral and physiologic state of the mouse. *Psychopharmacologia* **13**, 222–257.
74 Pollak D, Weitzdoerfer R, Yang YW, Prast H, Hoeger H & Lubec G (2005) Cerebellar protein expression in three different mouse strains and their relevance for motor performance. *Neurochem Int* **46**, 19–29.
75 Bailey KR & Crawley JN (2009) Anxiety-related behaviors in mice. In Methods of Behavior Analysis in Neuroscience (JJ B, ed), CRC Press, Boca Raton, FL.
76 O'Mahony CM, Sweeney FF, Daly E, Dinan TG & Cryan JF (2010) Restraint stress-induced brain activation patterns in two strains of mice differing in their anxiety behaviour. *Behav Brain Res* **213**, 148–154.
77 Weitzdoerfer R, Hoeger H, Engidawork E, Engelmann M, Singewald N, Lubec G & Lubec B (2004) Neuronal nitric oxide synthase knock-out mice show impaired cognitive performance. *Nitric Oxide* **10**, 130–140.
78 Ibarguen-Vargas Y, Surget A, Vourc'h P, Leman S, Andres CR, Gardier AM & Belzung C (2009) Deficit in BDNF does not increase vulnerability to stress but dampens antidepressant-like effects in the unpredictable chronic mild stress. *Behav Brain Res* **202**, 245–251.
79 Kong E, Sucic S, Monje FJ, Savalli G, Diao W, Khan D, Ronovsky M, Cabatic M, Koban F, Freissmuth M *et al.* (2015) STAT3 controls IL6-dependent regulation of serotonin transporter function and depression-like behavior. *Sci Rep* **5**, 9009.
80 Monje FJ, Cabatic M, Divisch I, Kim EJ, Herkner KR, Binder BR & Pollak DD (2011) Constant darkness induces IL-6-dependent depression-like behavior through the NF-kappaB signaling pathway. *J Neurosci* **31**, 9075–9083.
81 Savalli G, Diao W, Berger S, Ronovsky M, Partonen T & Pollak DD (2015) Anhedonic behavior in cryptochrome 2-deficient mice is paralleled by altered diurnal patterns of amygdala gene expression. *Amino Acids* **47**, 1367–1377.
82 Laursen H & Westergaard E (1981) The permeability of the blood-brain barrier and cell membranes to horseradish peroxidase in hyperammonaemia. *Acta Neuropathol* **54**, 293–299.